

# Reactions of a phosphido-bridged unsymmetrical diiron complex ( $\eta^5\text{-C}_5\text{Me}_5\text{Fe}_2(\text{CO})_4(\mu\text{-CO})(\mu\text{-PPh}_2)$ ) with various alkynes

Hisako Hashimoto <sup>a,\*</sup>, Kazuyoshi Kurashima <sup>a</sup>, Hiromi Tobita <sup>a,\*</sup>, Hiroshi Ogino <sup>b</sup>

<sup>a</sup> Department of Chemistry, Graduate School of Science, Tohoku University, Aoba-ku, Aramaki, Aoba, Sendai 980-8578, Japan

<sup>b</sup> Miyagi Study Center, The University of the Air, Sendai 980-8577, Japan

Received 2 December 2003; accepted 8 January 2004

## Abstract

A phosphido-bridged unsymmetrical diiron complex ( $\eta^5\text{-C}_5\text{Me}_5\text{Fe}_2(\text{CO})_4(\mu\text{-CO})(\mu\text{-PPh}_2)$  (**1**) was synthesized by a new convenient method; photo-dissociation of a CO ligand from ( $\eta^5\text{-C}_5\text{Me}_5\text{Fe}_2(\text{CO})_6(\mu\text{-PPh}_2)$  (**2**) that was prepared by the reaction of  $\text{Li}[\text{Fe}(\text{CO})_4\text{PPh}_2]$  with ( $\eta^5\text{-C}_5\text{Me}_5\text{Fe}(\text{CO})_2\text{I}$ ). The reactivity of **1** toward various alkynes was studied. The reaction of **1** with  $\text{tBuC}\equiv\text{CH}$  gave a 1:1 mixture of two isomeric complexes ( $\eta^5\text{-C}_5\text{Me}_5\text{Fe}_2(\text{CO})_3(\mu\text{-PPh}_2)[\mu\text{-CH}=\text{C}(\text{tBu})\text{C}(\text{O})]$  (**3**) containing a ketoalkenyl ligand. The reactions of **1** with other terminal alkynes  $\text{RC}\equiv\text{CH}$  ( $\text{R} = \text{H}, \text{CO}_2\text{Me}, \text{Ph}$ ) afforded complexes incorporating one or two molecules of alkynes and a carbonyl group. The principal products were dinuclear complexes bridged by a new phosphinoketoalkenyl ligand, ( $\eta^5\text{-C}_5\text{Me}_5\text{Fe}_2(\text{CO})_3(\mu\text{-CO})[\mu\text{-CR}^1=\text{CR}^2\text{C}(\text{O})\text{PPh}_2]$  (**4a**:  $\text{R}^1 = \text{H}, \text{R}^2 = \text{H}$ ; **4b**:  $\text{R}^1 = \text{CO}_2\text{Me}, \text{R}^2 = \text{H}$ ; **4c**:  $\text{R}^1 = \text{H}, \text{R}^2 = \text{Ph}$ ). In the cases of alkynes  $\text{RC}\equiv\text{CH}$  ( $\text{R} = \text{H}, \text{CO}_2\text{Me}$ ), dinuclear complexes having a new ligand composed of two molecules of alkynes, a carbonyl group, and a phosphido group; i.e. ( $\eta^5\text{-C}_5\text{Me}_5\text{Fe}_2(\text{CO})_3[\mu\text{-CRCHCHCRC}(\text{O})\text{PPh}_2]$  (**5a**:  $\text{R} = \text{H}$ ; **5b**:  $\text{R} = \text{CO}_2\text{Me}$ ), were also obtained. In all cases, mononuclear complexes, ( $\eta^5\text{-C}_5\text{Me}_5\text{Fe}(\text{CO})[\text{CR}^1=\text{CR}^2\text{C}(\text{O})\text{PPh}_2]$  (**6a**:  $\text{R}^1 = \text{H}, \text{R}^2 = \text{H}$ ; **6b**:  $\text{R}^1 = \text{H}, \text{R}^2 = \text{CO}_2\text{Me}$ ; **6c**:  $\text{R}^1 = \text{H}, \text{R}^2 = \text{Ph}$ ) were isolated in low yields. The structures of **1**, **4c**, **5b**, and **6a** were confirmed by X-ray crystallography. The detailed structures of the products and plausible reaction mechanisms are discussed. © 2004 Elsevier B.V. All rights reserved.

**Keywords:** Iron complex; Phosphido-bridged complex; Alkyne insertion; C–C bond formation; P–C bond formation; X-ray structure analysis

## 1. Introduction

The chemistry of dinuclear transition-metal complexes continues to attract considerable interests owing to its unique activation of substrates, so-called “bimetallic activation”, which cannot be expected to mononuclear complexes [1]. Multisite interactions between the metal aggregates and substrate molecules followed by their activation are often believed to operate during chemical transformations, but not fully understood. In relation to this, we have been interested in homometallic but unsymmetrical dinuclear complexes where each metal has the different supporting ligands. This type of complexes are much less studied among a large number of dinuclear complexes, and are expected to be suited to

spotlight the difference of the effects of ligands bound to the neighboring metals during bimetallic activation.

We previously reported the synthesis of a phosphido-bridged unsymmetrical diiron complex ( $\eta^5\text{-C}_5\text{Me}_5\text{Fe}_2(\text{CO})_4(\mu\text{-CO})(\mu\text{-PPh}_2)$  (**1**) [2]. Complex **1** shows a unique reactivity toward hydrosilanes to cause the stoichiometric redistribution of dihydrosilane to produce monohydrosilane and a monohydrosilylene-bridged diiron complex [3a], and the catalytic redistribution of trihydrosilane to produce dihydrosilane and tetrahydrosilane [3b]. In these reactions, the steric difference of the ligands between two metal atoms seems to play an important role to control the route of reaction. For our continuous interests about reactivity of this type of unsymmetrical complexes, we studied the reactions of **1** with various alkynes and found that one or two alkynes and a carbonyl group inserted into one of the Fe–P bonds of the bridging phosphido ligand regioselectively to produce new complexes having a ligand with a

\* Corresponding authors. Tel.: +81222176540; fax: +81222176543.

E-mail address: hhashimoto@mail.tains.tohoku.ac.jp (H. Hashimoto).

–P–C(O)– CR′=CR– or –P–C(O)CR′=CR′CR=CR′– linkage dependent on the substituents on the alkynes. There are now an increasing number of reports for alkyne and/or CO insertion into the bond between the metal and the bridging phosphido ligand in dinuclear complexes [4–8]. For example, Werner et al. [8] reported an insertion of Me<sub>2</sub>OOC≡CCO<sub>2</sub>Me into the Co–P bond in (η<sup>5</sup>-C<sub>5</sub>H<sub>5</sub>)<sub>2</sub>Co<sub>2</sub>(μ-PMe<sub>2</sub>)<sub>2</sub> to produce a dinuclear complex with an alkenylphosphine ligand. Mays et al. [5] reported that the ring expansion underwent by the reactions of Co<sub>2</sub>(CO)<sub>6</sub>(μ-PPh<sub>2</sub>) with alkynes to afford complexes bearing a ligand such as μ-PPh<sub>2</sub>CR=CR′C(O) and μ-PPh<sub>2</sub>CR=CR′C(O)CR″=CR′″. Yamazaki et al. [6] and Dixneuf et al. [7] also reported the alkyne-insertion reactions by using heterometallic phosphido-bridged complexes. These examples well demonstrated the existence of the new methodology of the P–C bond formation using dinuclear complexes, though the detailed mechanisms and the controlling factors of the product formation have not been clarified yet.

We report here the new convenient preparation, the X-ray structure, and the details of the reactions of **1** with various alkynes and propose the reaction mechanisms for our system.

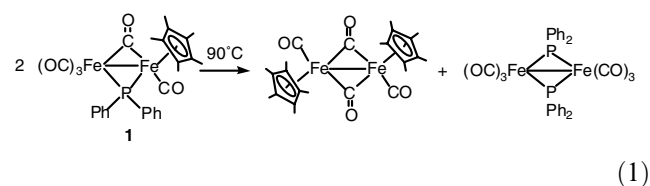
## 2. Results and discussion

### 2.1. A new preparation and X-ray structure determination of (η<sup>5</sup>-C<sub>5</sub>Me<sub>5</sub>)Fe<sub>2</sub>(CO)<sub>4</sub>(μ-CO)(μ-PPh<sub>2</sub>) (**1**)

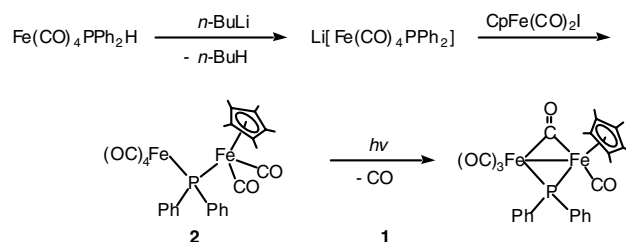
Complex **1** was first synthesized by us by the reaction of a tetramethylfulvene-bridged diiron complex (η<sup>1</sup>:η<sup>5</sup>-CH<sub>2</sub>C<sub>5</sub>Me<sub>4</sub>)Fe<sub>2</sub>(CO)<sub>6</sub> with diphenylphosphine [2]. As this method needed several steps from the starting pentamethylcyclopentadiene, we started to search a simpler synthetic method by referring to those of other related complexes. The cyclopentadienyl analog of **1**, (η<sup>5</sup>-C<sub>5</sub>H<sub>5</sub>)Fe<sub>2</sub>(CO)<sub>4</sub>(μ-CO)(μ-PPh<sub>2</sub>), has previously been synthesized by three methods. Haines and co-workers [9] reported that the reaction of Na-[(η<sup>5</sup>-C<sub>5</sub>H<sub>5</sub>)Fe(CO)<sub>2</sub>] with Fe(CO)<sub>4</sub>(PPh<sub>2</sub>Cl) gave (η<sup>5</sup>-C<sub>5</sub>H<sub>5</sub>)Fe<sub>2</sub>(CO)<sub>6</sub>(μ-PPh<sub>2</sub>), which then underwent photochemical CO dissociation to produce the cyclopentadienyl analog of **1**. They also reported that the complex (η<sup>5</sup>-C<sub>5</sub>H<sub>5</sub>)Fe<sub>2</sub>(CO)<sub>6</sub>(μ-PPh<sub>2</sub>) was obtained by the reaction of Fe<sub>2</sub>(CO)<sub>9</sub> with (η<sup>5</sup>-C<sub>5</sub>H<sub>5</sub>)Fe(CO)<sub>2</sub>(PPh<sub>2</sub>) in 80% yield [9]. Yasufuku and Yamazaki prepared the same complex (η<sup>5</sup>-C<sub>5</sub>H<sub>5</sub>)Fe<sub>2</sub>(CO)<sub>6</sub>(μ-PPh<sub>2</sub>) in 40% yield from the reaction of (η<sup>5</sup>-C<sub>5</sub>H<sub>5</sub>)Fe(CO)<sub>2</sub>Cl with Fe(CO)<sub>4</sub>(PPh<sub>2</sub>H) in the presence of HNEt<sub>2</sub>. It was then converted to (η<sup>5</sup>-C<sub>5</sub>H<sub>5</sub>)Fe<sub>2</sub>(CO)<sub>4</sub>(μ-CO)(μ-PPh<sub>2</sub>) in 70% yield in a similar photochemical method [10].

As modification of these methods, we newly developed a convenient method to prepare **1**, which is shown

in Scheme 1. Thus, the deprotonation of hydrophosphine iron complex Fe(CO)<sub>4</sub>(PPh<sub>2</sub>H) with *n*-BuLi produced the anionic complex Li[Fe(CO)<sub>4</sub>PPh<sub>2</sub>], which was then treated with (η<sup>5</sup>-C<sub>5</sub>Me<sub>5</sub>)Fe(CO)<sub>2</sub>I to give (η<sup>5</sup>-C<sub>5</sub>Me<sub>5</sub>)Fe<sub>2</sub>(CO)<sub>6</sub>(μ-PPh<sub>2</sub>) (**2**) in 97% yield. Subsequent photochemical CO dissociation from **2** produced **1** in 76% yield. The <sup>31</sup>P NMR signal of **2** appears at 90.8 ppm (in C<sub>6</sub>D<sub>6</sub>), which lies much higher in field compared with that of **1** (169.9 ppm). These data and comparison of them with the previous examples suggest that **2** does not have a metal–metal bond whereas **1** has a metal–metal bond [11]. For example, the <sup>31</sup>P NMR signals of (η<sup>5</sup>-C<sub>5</sub>H<sub>5</sub>)Fe(CO)<sub>2</sub>(μ-PPh<sub>2</sub>)W(CO)<sub>5</sub> (with no metal–metal bond) and (η<sup>5</sup>-C<sub>5</sub>H<sub>5</sub>)Fe(CO)(μ-CO)(μ-PPh<sub>2</sub>)W(CO)<sub>4</sub> (with a metal–metal bond) are reported to appear at 0.1 and 160.8 ppm (in THF), respectively [12a]. Complex **1** is inert to UV light, but thermally decomposes above 90 °C to produce (η<sup>5</sup>-C<sub>5</sub>Me<sub>5</sub>)<sub>2</sub>Fe<sub>2</sub>(CO)<sub>4</sub> and Fe<sub>2</sub>(CO)<sub>6</sub>(μ-PPh<sub>2</sub>)<sub>2</sub> quantitatively as described in the following equation



Although the crystal structures of several unsymmetrical monophosphido-bridged dinuclear complexes with one cyclopentadienyl group have been determined [11–14], those of (η<sup>5</sup>-C<sub>5</sub>Me<sub>5</sub>)Fe<sub>2</sub>(CO)<sub>4</sub>(μ-CO)(μ-PPh<sub>2</sub>) (**1**) and its η<sup>5</sup>-C<sub>5</sub>H<sub>5</sub> analog have not been determined. Therefore, we performed the X-ray crystal structure determination of **1**. Black needle-like crystals of **1** suitable for X-ray analysis were obtained by layering a toluene solution of **1** with hexane at –15 °C. Two independent molecules (A and B) were found in the unit cell. The molecular structures of them are illustrated in Fig. 1, and crystal data and structure refinement information are presented in Table 1. The selected interatomic distances and bond angles are given in Table 2 together with the mean values. The two molecules differ in the orientation of the phenyl groups on the phosphido ligand with marginally different bonding parameters,



Scheme 1.

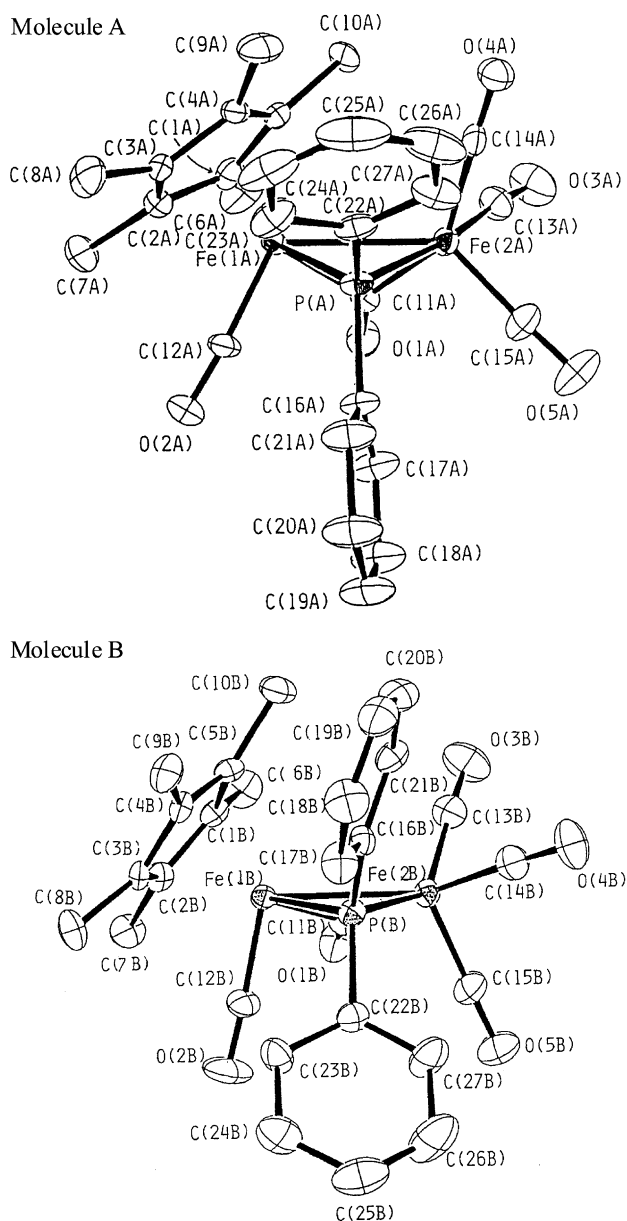


Fig. 1. ORTEP drawing of  $(\eta^5\text{-C}_5\text{Me}_5)\text{Fe}_2(\text{CO})_4(\mu\text{-CO})(\mu\text{-PPh}_2)$  (**1**), showing 50% thermal ellipsoids. Hydrogen atoms were omitted for clarity.

but the whole features are essentially equal to each other. Therefore, the mean values of the two molecules are used in the following discussion. The two iron atoms are bridged by a phosphido and a carbonyl group. The Fe(1) atom adopts an almost four-legged piano-stool structure and the Fe(2) atom adopts a distorted octahedral structure. The average Fe–Fe bond distance is 2.643(2) Å, which is slightly longer than that in  $(\eta^5\text{-C}_5\text{H}_5)\text{Fe}_2(\text{CO})_4(\mu\text{-CO})(\mu\text{-PMe}_2)$  (av. 2.627(2) Å) [14b], but in the range of normal single bond lengths found in other phosphido-bridged complexes; e.g. 2.623(3) Å for  $\text{Fe}_2(\text{CO})_6(\mu\text{-PPh}_2)_2$  [15], 2.662(1) Å for  $\text{Fe}_2(\text{CO})_6(\mu\text{-PPhH})_2$  [15], and av. 2.610(3) Å for  $\text{Fe}_2(\text{CO})_6(\mu\text{-PPh}_2)(\mu\text{-SPh})$  [16]. Both of the bridging phosphido and carbonyl ligands are almost symmetrically coordinated to the two iron atoms (av. 2.208(3) Å for Fe(1)–P, av. 2.207(3) Å for Fe(2)–P; and av. 1.969(9) Å for Fe(1)–C(O), av. 1.944(11) Å for Fe(2)–C(O)), despite differences in adjacent ligands and oxidation numbers [+2 for Fe(1), 0 for Fe(2)] between the two metals. The Fe–P bond distances and the angle Fe(1)–P–Fe(2) (av. 73.54(9)°) of **1** are comparable with the corresponding values of other related complexes: the Fe–P bond lengths, 2.233(3) Å for  $\text{Fe}_2(\text{CO})_6(\mu\text{-PPh}_2)_2$  [15], av. 2.203(3) and 2.184(3) Å for  $(\eta^5\text{-C}_5\text{H}_5)\text{Fe}_2(\text{CO})_4(\mu\text{-CO})(\mu\text{-PMe}_2)$  [14b], av. 2.212(1) Å for  $\text{Fe}_2(\text{CO})_6(\mu\text{-PPhH})_2$  [15]; the Fe–P–Fe bond angles, 72.0(1)° for  $\text{Fe}_2(\text{CO})_6(\mu\text{-PPh}_2)_2$  [15], av. 73.6(1)° for  $(\eta^5\text{-C}_5\text{H}_5)\text{Fe}_2(\text{CO})_4(\mu\text{-CO})(\mu\text{-PMe}_2)$  [14b], 74.0(1)° for  $\text{Fe}_2(\text{CO})_6(\mu\text{-PPhH})_2$  [15]. These structural features are almost identical to those of  $(\eta^5\text{-C}_5\text{H}_5)\text{Fe}_2(\text{CO})_4(\mu\text{-CO})(\mu\text{-PMe}_2)$ , but there is a significant steric repulsion between a bulky  $\eta^5\text{-C}_5\text{Me}_5$  group and a phenyl group on the bridging phosphido ligand in **1**: e.g. the distances of C(9)···C(22) and C(9)···C(23) in molecule A are 3.52(2) and 3.53(2) Å, respectively, which are shorter than the sum of the effective van der Waals radii of a methyl group and a half-thickness of the  $\pi$ -cloud of a phenyl group (3.7 Å). Similar steric repulsions are also observed in molecule B: the short distances between a methyl carbon of the  $\eta^5\text{-C}_5\text{Me}_5$  ring and some of the phenyl carbon atoms are 3.32(1) Å for C(9)···C(16), 3.56(1) Å for C(9)···C(21), and 3.61(1) Å for C(10)···C(21), respectively.

## 2.2. Reactions of **1** with alkynes and characterizations of the products

The phosphido-bridged diiron complex **1** reacted with  $t\text{BuC}\equiv\text{CH}$  at 35 °C to give  $(\eta^5\text{-C}_5\text{Me}_5)\text{Fe}_2(\text{CO})_3(\mu\text{-PPh}_2)[\mu\text{-CH=C}(t\text{Bu})\text{C}(\text{O})]$  (**3**) containing a new ketoalkenyl ligand in 59% yield (Eq. (2)). Although we have not succeeded in growing crystals of **3** suitable for X-ray diffraction study, **3** was characterized spectroscopically (Table 3) [17]. All spectral data suggest that there are two isomeric complexes for **3**, which are in equilibrium in solution (see experimental section). Knox et al. [18] also reported that their isomeric complexes having a similar  $\mu$ -ketoalkenyl ligand,  $\text{Fe}_2(\text{CO})_5\{\mu\text{-CR}^1\text{=CR}^2\text{C}(\text{O})\}(\mu\text{-dppm})$  ( $\text{R}^1 = \text{H}$ ,  $\text{R}^2 = \text{Me}$ ;  $\text{R}^1 = \text{H}$ ,  $\text{R}^2 = \text{Ph}$ ) are in equilibrium in solution. Therefore, we suggest that the two isomers have the *syn*- and *anti*-configurations with respect to the mutual positions of the  $\eta^5\text{-C}_5\text{Me}_5$  ligand and the carbonyl group of the ketoalkenyl ligand as displayed in Chart 1. In the  $^{31}\text{P}$  NMR spectrum, two sets of signals for **3** appear at very low field, 257.6 and 265.3 ppm, which suggests that both

Table 1  
Crystallographic data for complexes **1**, **4c**, **5b**, and **6a**

Entry	<b>1</b>	<b>4c</b>	<b>5b</b>	<b>6a</b>
Formula	C <sub>27</sub> H <sub>25</sub> Fe <sub>2</sub> O <sub>5</sub> P	C <sub>35</sub> H <sub>31</sub> Fe <sub>2</sub> O <sub>5</sub> P·3/ 2C <sub>7</sub> H <sub>8</sub>	C <sub>34</sub> H <sub>33</sub> Fe <sub>2</sub> O <sub>8</sub> P	C <sub>26</sub> H <sub>27</sub> FeO <sub>2</sub> P
Fw	572.17	812.51	712.3	458.3
Crystal system	Triclinic	Monoclinic	Monoclinic	Triclinic
Space group	$P\bar{1}$ (No. 2)	$A2/n$ (No. 15)	$P_1/a$ (No. 14)	$P\bar{1}$ (No. 2)
<i>a</i> (Å)	15.205(2)	36.102(6)	25.148(4)	14.501(2)
<i>b</i> (Å)	19.863(5)	11.865(1)	10.841(2)	18.825(4)
<i>c</i> (Å)	19.863(5)	17.960(4)	11.683(2)	8.666(1)
$\alpha$ (°)	109.44(2)			100.93(2)
$\beta$ (°)	99.71(2)	94.13(1)	100.09(1)	91.54(1)
$\gamma$ (°)	76.29(2)			78.68(2)
<i>V</i> (Å <sup>3</sup> )	2598(1)	7673(2)	3135.6(9)	2277.4(6)
<i>Z</i>	4	8	4	4
$\rho_{\text{calcd}}$ (g cm <sup>-3</sup> )	1.46	1.41	1.51	1.34
$\mu$ (Mo K $\alpha$ ) (cm <sup>-1</sup> )	6.20	4.20	10.55	7.71
Crystal size (mm)	0.14 × 0.25 × 0.40	0.40 × 0.30 × 0.35	0.30 × 0.15 × 0.25	0.52 × 0.38 × 0.10
Radiation	Mo K $\alpha$ ( <i>l</i> = 0.71073 Å)	Mo K $\alpha$ ( <i>l</i> = 0.71073 Å)	Mo K $\alpha$ ( <i>l</i> = 0.71073 Å)	Mo K $\alpha$ ( <i>l</i> = 0.71073 Å)
Monochromator	Graphite	Graphite	Graphite	Graphite
<i>T</i> (°C)	18	18	20	20
Reflections measured	$\pm h, \pm k, l$	$\pm h, k, l$	$\pm h, k, l$	$\pm h, \pm k, l$
2 $\theta$ range (°)	3–53	3–55	3–50	3–50
scan mode	$\omega$ -2 $\theta$	$\omega$	$\omega$	$\omega$ -2 $\theta$
$\omega$ -scan width (°)	1.1 + 0.35 tan $\theta$	1.2 + 0.35 tan $\theta$	1.1 + 0.35 tan $\theta$	1.1 + 0.35 tan $\theta$
No. of unique data	10746	12740	5843	8016
No. of data used	6186 ( $ F_o  > 3\sigma( F_o )$ )	3165 ( $ F_o  > 6\sigma( F_o )$ )	3337 ( $ F_o  > 3\sigma( F_o )$ )	5388 ( $ F_o  > 3\sigma( F_o )$ )
No. of parameters refined	417	499	415	542
<i>R</i> <sup>a</sup>	0.069	0.057	0.068	0.075
<i>R</i> <sub>w</sub> <sup>b</sup>	0.076	0.071	A0.089	0.092
Quality of fit indicator <sup>c</sup>	1.28	1.39	1.36	1.66
Maximum residual electron density (e Å <sup>-3</sup> )	0.86	0.50	0.79	0.73

<sup>a</sup>  $R = \sum(|F_o| - |F_c|) / \sum|F_o|$ .

<sup>b</sup>  $R_w = [\sum_w(|F_o| - |F_c|)^2 / \sum_w|F_o|^2]^{1/2}$ ;  $w = [\sigma_2^2(|F_o|) + aF_o^{21}]^{-1}$ , where  $a = 0.001$  for complexes **1** and **6a**, and  $a = 0.003$  for complexes **4c** and **5b**.

<sup>c</sup>  $[\sum(|F_o| - |F_c|)^2 / (N_{\text{observations}} - N_{\text{parameters}})]^{1/2}$ .

of them have a phosphido ligand bridging across the metal–metal bond [11]. The mass spectrum (FAB) of the mixture shows the  $M^+ + 1$  at  $m/z = 627$  along with

Table 2  
Selected bond distances (Å) and angles (°) for ( $\eta^5$ -C<sub>5</sub>Me<sub>5</sub>)Fe<sub>2</sub>(CO)<sub>4</sub>( $\mu$ -CO)( $\mu$ -PPH<sub>2</sub>) (**1**)

	Molecule A (X = A)	Molecule B (X = B)	Average
<i>Bond distances</i>			
Fe(1X)–Fe(2X)	2.643(2)	2.651(2)	2.643(2)
Fe(1X)–P(X)	2.224(2)	2.191(3)	2.208(3)
Fe(2X)–P(X)	2.210(2)	2.203(3)	2.207(3)
Fe(1X)–C(11X)	1.990(9)	1.948(9)	1.969(9)
Fe(2X)–C(11X)	1.932(7)	1.956(11)	1.944(11)
Fe(1X)–C(12X)	1.740(10)	1.759(10)	1.750(10)
<i>Bond angles</i>			
Fe(1X)–Fe(2X)–P(X)	53.82(6)	53.10(7)	53.5(7)
Fe(2X)–Fe(1X)–P(X)	53.30(6)	52.69(6)	53.0(6)
Fe(1X)–P(X)–Fe(2X)	72.88(7)	74.20(9)	73.54(9)
Fe(1X)–Fe(2X)–C(11X)	48.8(2)	47.4(3)	48.1(3)
Fe(2X)–Fe(1X)–C(11X)	46.9(3)	47.1(3)	47.0(3)
Fe(1X)–C(11X)–Fe(2X)	84.4(3)	85.5(5)	85.0(5)

the fragment peaks corresponding to the successive loss of four carbonyls. A proton resonance for the  $\mu$ -CH portion of each of two isomers appears at very low field [10.72 ppm ( $^3J_{\text{PH}} = 0.7$  Hz) and 11.14 ppm ( $^3J_{\text{PH}} = 1.2$  Hz)] that is characteristic of the bridging carbene proton. In accord with this, two sets of the <sup>13</sup>C NMR signals for  $\mu$ -CH carbons of the isomers appear at 185.1 ppm ( $^2J_{\text{PC}} = 4.2$  Hz) and 189.3 ppm ( $^2J_{\text{PC}} = 3.4$  Hz), which are in the typical region of the bridging carbene carbons. Two resonances at 70.8 ppm ( $^3J_{\text{PC}} = 2.6$  Hz) and 77.8 ppm ( $^3J_{\text{PC}} = 2.6$  Hz) can be assigned to two sets of alkenyl carbon signals for the =C(<sup>t</sup>Bu)C(O)– moiety. There are eight doublets in a carbonyl region for two isomers. Two of them must come from the inserted carbonyls in the new bridging ligands, though the exact assignments of them are difficult. A clear evidence for the existence of the inserted carbonyls comes from the IR spectrum (KBr pellet). In addition to the  $\nu_{\text{CO}}$  bands for the terminal carbonyls, several  $\nu_{\text{CO}}$  bands appear around 1700 cm<sup>-1</sup>, which is typical of a ketoalkenyl carbon, assigned to the inserted carbonyl groups. The

Table 3  
<sup>1</sup>H NMR, <sup>31</sup>P NMR, and IR spectral data for complexes 3–6

Complex	$\delta_{\text{H}}^{\text{a}}$	$\delta_{\text{P}}^{\text{b}}$	$\nu(\text{CO})^{\text{d}}$
<b>3</b> , ( $\eta^5\text{-C}_5\text{Me}_5$ )Fe <sub>2</sub> (CO) <sub>3</sub> ( $\mu\text{-PPh}_2$ )=[ $\mu\text{-CH=C}(\text{tBu})\text{C}(\text{O})$ ] (a mixture of two isomers)	1.20 (s, 15H, C <sub>5</sub> Me <sub>5</sub> ), 1.30 (s, 15H, C <sub>5</sub> Me <sub>5</sub> ) 1.27 (s, 9H, tBu), 1.31 (s, 9H, tBu), 6.9–8.2 (m, 10H, Ph), 10.72 (d, <sup>3</sup> J <sub>PH</sub> = 0.7 Hz, $\mu\text{-CH}$ ), 11.14 (d, <sup>3</sup> J <sub>PH</sub> = 1.2 Hz, $\mu\text{-CH}$ )	257.6 <sup>c</sup> , 265.3 <sup>c</sup>	1983vs, 1959vs, 1950vs, 1907vs, 1732s, 1699m, 1686s
<b>4a</b> , ( $\eta^5\text{-C}_5\text{Me}_5$ )Fe <sub>2</sub> (CO) <sub>3</sub> ( $\mu\text{-CO}$ )=[ $\mu\text{-CH=CHC}(\text{O})\text{PPh}_2$ ]	(1.25 s, 15H, C <sub>5</sub> Me <sub>5</sub> ), 4.24 (dd, <sup>3</sup> J <sub>PH</sub> = 31.8 Hz, <sup>3</sup> J <sub>HH</sub> = 4.8 Hz, 1H, $-\text{CHC}(\text{O})-$ ), 6.8–8.2 (m, 10H, Ph), 9.92 (dd, <sup>3</sup> J <sub>PH</sub> = 2.4 Hz, <sup>3</sup> J <sub>HH</sub> = 4.8 Hz, 1H, $\mu\text{-CH}$ ),	75.3	2015vs, 1942vs, 1924s, 1843m, 1635m, 1624m
<b>4b</b> , ( $\eta^5\text{-C}_5\text{Me}_5$ )Fe <sub>2</sub> (CO) <sub>3</sub> ( $\mu\text{-CO}$ )=[ $\mu\text{-C}(\text{CO}_2\text{Me})=\text{CHC}(\text{O})\text{PPh}_2$ ]	1.38 (s, 15H, C <sub>5</sub> Me <sub>5</sub> ) 3.73 (s, 3H, CO <sub>2</sub> Me), 4.18 (d, <sup>3</sup> J <sub>PH</sub> = 34.7 Hz, 1H, CCH), 6.8–8.3 (m, 10H, Ph)	56.4,	2040vs, 2017s, 1975vs, 1900m, 1869s, 1682m, 1624s
<b>4c</b> , ( $\eta^5\text{-C}_5\text{Me}_5$ )Fe <sub>2</sub> (CO) <sub>3</sub> ( $\mu\text{-CO}$ )=[ $\mu\text{-CH=CPhC}(\text{O})\text{PPh}_2$ ]	1.34 (s, 15H, C <sub>5</sub> Me <sub>5</sub> ), 6.5–8.2 (m, 15H, Ph), 10.81 (d, <sup>3</sup> J <sub>PH</sub> = 2.0 Hz, 1H, CH)	81.5,	2013vs, 1959vs, 1936vs, 1924vs, 1857m, 1589m
<b>5a</b> , ( $\eta^5\text{-C}_5\text{Me}_5$ )Fe <sub>2</sub> (CO) <sub>3</sub> =[ $\mu\text{-CH-CHCHCH-C}(\text{O})\text{PPh}_2$ ]	1.34 (s, 15H, C <sub>5</sub> Me <sub>5</sub> ), 4.01 (br, t, <sup>3</sup> J <sub>HH</sub> = 8.4 Hz, 1H, CH), 4.93 (dd, <sup>3</sup> J <sub>HH</sub> = 8.4 Hz, <sup>3</sup> J <sub>PH</sub> = 23.6 Hz, 1H, $-\text{CHC}(\text{O})$ ), 5.02 (br, t, <sup>3</sup> J <sub>HH</sub> = 8.4 Hz, 1H, CH), 6.8–7.7 (m, 10H, Ph), 8.79 (br, d, <sup>3</sup> J <sub>HH</sub> = 8.4 Hz, 1H, $\mu\text{-CH}$ )	57.5	2013s, 1942vs, 1925s, 1832m, 1635m
<b>5b</b> , ( $\eta^5\text{-C}_5\text{Me}_5$ )Fe <sub>2</sub> (CO) <sub>3</sub> =[ $\mu\text{-C}(\text{CO}_2\text{-Me})\text{CHCHCC}(\text{CO}_2\text{Me})\text{C}(\text{O})\text{PPh}_2$ ]	(C <sub>6</sub> D <sub>6</sub> ): 0.96 (s, 15H, C <sub>5</sub> Me <sub>5</sub> ), 3.43 (s, 3H, CO <sub>2</sub> Me), 3.63 (dd, <sup>3</sup> J <sub>HH</sub> = 4.0 Hz, <sup>3</sup> J <sub>PH</sub> = 2.1 Hz, 1H, CH), 3.77 (s, 3H, CO <sub>2</sub> Me), 6.27 (dd, <sup>3</sup> J <sub>HH</sub> = 4.0 Hz, <sup>3</sup> J <sub>PH</sub> = 1.5 Hz, 1H, CH), 6.8–8.2 (m, 10H, Ph)	(C <sub>6</sub> D <sub>6</sub> ) 75.9,	2037vs, 1969vs, 1711m, 1693s, 1687s, 1647m, 1637w
<b>6a</b> , ( $\eta^5\text{-C}_5\text{Me}_5$ )Fe(CO)[CH=CHC(O)PPh <sub>2</sub> ]	(CD <sub>2</sub> Cl <sub>2</sub> ): 1.31 (s, 15H, C <sub>5</sub> Me <sub>5</sub> ), 3.45 (s, 3H, CO <sub>2</sub> Me), 3.48 (dd, <sup>3</sup> J <sub>HH</sub> = 4.0 Hz, <sup>3</sup> J <sub>PH</sub> = 2.2 Hz, 1H, CH), 4.05 (s, 3H, CO <sub>2</sub> Me), 6.20 (dd, <sup>3</sup> J <sub>HH</sub> = 4.0 Hz, <sup>3</sup> J <sub>PH</sub> = 1.6 Hz, 1H, CH), 7.4–8.0 (m, 10H, Ph) 1.34 (d, <sup>4</sup> J <sub>PH</sub> = 0.5 Hz, 15H, C <sub>5</sub> Me <sub>5</sub> ), 6.8–8.3 (m, 10H, Ph), 7.63 (dd, <sup>3</sup> J <sub>HH</sub> = 7.7 Hz, <sup>3</sup> J <sub>PH</sub> = 35.0 Hz, 1H, =CHC(O)-), 10.82 (dd, <sup>3</sup> J <sub>HH</sub> = 7.7 Hz, <sup>3</sup> J <sub>PH</sub> = 2.5 Hz, 1H, Fe-CH=)	(CD <sub>2</sub> Cl <sub>2</sub> ) 79.0	1919vs, 1720s, 1637w
<b>6b</b> , ( $\eta^5\text{-C}_5\text{Me}_5$ )Fe(CO)-[CH=C(CO <sub>2</sub> Me)C(O)PPh <sub>2</sub> ]	1.29 (s, 15H, C <sub>5</sub> Me <sub>5</sub> ), 3.60 (s, 3H, CO <sub>2</sub> Me), 6.7–8.2 (m, 10H, Ph), 12.81 (d, <sup>3</sup> J <sub>PH</sub> = 0.5 Hz, 1H, CH)	88.6	1942vs, 1720m, 1691w, 1625m
<b>6c</b> , ( $\eta^5\text{-C}_5\text{Me}_5$ )Fe(CO)-[CH=CPhC(O)PPh <sub>2</sub> ]	1.37 (s, 15H, C <sub>5</sub> Me <sub>5</sub> ), 6.8–8.3 (m, 15H, Ph), 11.39 (d, <sup>3</sup> J <sub>PH</sub> = 2.1 Hz, 1H, $\mu\text{-CH}$ )	87.1	1925vs, 1639s
<b>6d</b> , ( $\eta^5\text{-C}_5\text{Me}_5$ )Fe(CO)-[C(CO <sub>2</sub> Me)=C(CO <sub>2</sub> Me)C(O)PPh <sub>2</sub> ]	1.41 (s, 15H, C <sub>5</sub> Me <sub>5</sub> ), 3.04 (s, 3H, CO <sub>2</sub> Me), 3.45 (s, 3H, CO <sub>2</sub> Me), 6.8–8.3 (m, 10H, Ph),	107.0	1923vs, 1909vs, 1734vs, 1718s, 1593m, 1585m

<sup>a</sup> In C<sub>6</sub>D<sub>6</sub> at 300 MHz.

<sup>b</sup> In C<sub>6</sub>D<sub>6</sub> at 36.3 MHz, referenced to aqueous H<sub>3</sub>PO<sub>4</sub> (external).

<sup>c</sup> KBr pellet, cm<sup>-1</sup>.

<sup>d</sup> In C<sub>6</sub>D<sub>6</sub> at 121.5 MHz, referenced to aqueous H<sub>3</sub>PO<sub>4</sub> (external).

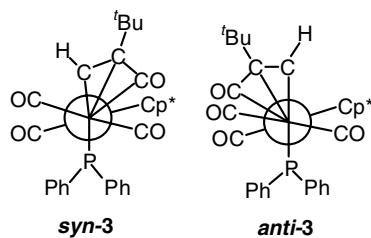
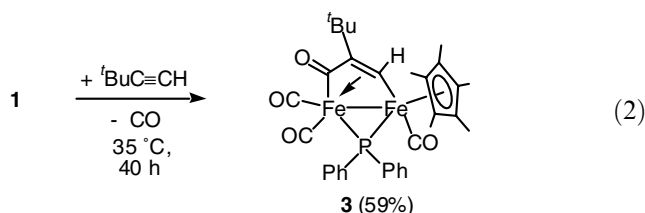


Chart 1.

observation of more than two bands in that region may be attributed to the packing effect of the crystals.



When complex **1** was treated with other terminal alkynes  $\text{RC}\equiv\text{CH}$  ( $\text{R} = \text{H}, \text{CO}_2\text{Me}, \text{Ph}$ ), complexes incorporating up to two molecules of alkynes were obtained (Eq. (3)). In every case, the principal product was a dinuclear complex incorporating one alkyne molecule in which the two iron atoms are bridged by a new phosphinoketoalkenyl ligand,  $(\eta^5\text{-C}_5\text{Me}_5)\text{Fe}_2(\text{CO})_3[\mu\text{-CO}][\mu\text{-CR}^1=\text{CR}^2\text{C}(\text{O})\text{PPh}_2]$  (**4a**:  $\text{R}^1 = \text{H}, \text{R}^2 = \text{H}$ ; **4b**:  $\text{R}^1 = \text{CO}_2\text{Me}, \text{R}^2 = \text{H}$ ; **4c**:  $\text{R}^1 = \text{H}, \text{R}^2 = \text{Ph}$ ). For  $\text{RC}\equiv\text{CH}$  ( $\text{R} = \text{CO}_2\text{Me}, \text{H}$ ), dinuclear complexes having a new ligand composed of two molecules of alkynes, a carbonyl group, and a phosphido group,  $(\eta^5\text{-C}_5\text{Me}_5)\text{Fe}_2(\text{CO})_3[\mu\text{-CR}^2\text{CR}^1\text{CR}^1\text{CR}^2\text{C}(\text{O})\text{PPh}_2]$  (**5a**:  $\text{R}^1 = \text{H}, \text{R}^2 = \text{H}$ ; **5b**:  $\text{R}^1 = \text{H}, \text{R}^2 = \text{CO}_2\text{Me}$ ), were also obtained. In all cases, mononuclear complexes,  $(\eta^5\text{-C}_5\text{Me}_5)\text{Fe}(\text{CO})_2[\text{CR}^1=\text{CR}^2\text{C}(\text{O})\text{PPh}_2]$  (**6a**:  $\text{R}^1 = \text{H}, \text{R}^2 = \text{H}$ ; **6b**:  $\text{R}^1 = \text{H}, \text{R}^2 = \text{CO}_2\text{Me}$ ; **6c**:  $\text{R}^1 = \text{H}, \text{R}^2 = \text{Ph}$ ) were isolated in low yields. The structures of **4c**, **5b**, and **6a** were confirmed by X-ray crystal structure analysis. Other complexes were fully characterized by comparing their spectral data with those of complexes **4c**, **5b**, and **6a**. Two regioisomers I and II depicted in Chart 2 are candidates for complexes **4b** and **4c**, but the repeated monitoring of the reaction of **1** with  $\text{PhC}\equiv\text{CH}$  by  $^1\text{H}$  NMR spectroscopy indicated the selective formation of

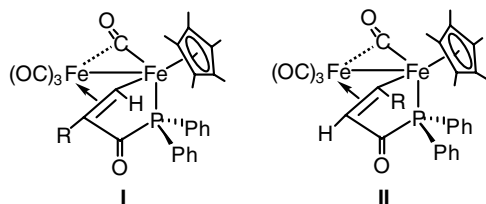
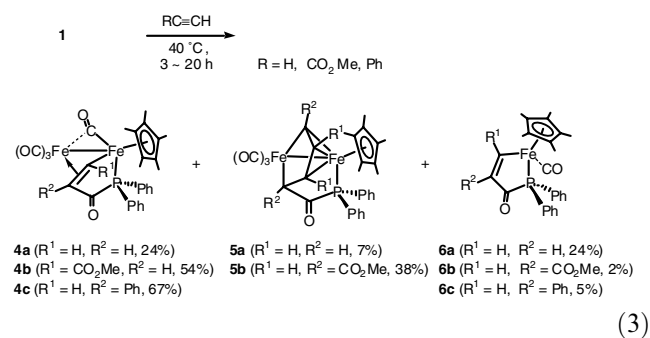


Chart 2.

**4c** with the structure of I. On the other hand, complex **4b** has the structure of II (vide infra). For the double alkyne-insertion product **5b**, four regioisomers are possible: a head-to-tail insertion leads to two isomers with a ligand having a  $-\text{CR}=\text{CH}-\text{CR}=\text{CH}-$  or  $-\text{CH}=\text{CR}-\text{CH}=\text{CR}-$  linkage, and a head-to-head insertion leads to two isomers containing a  $-\text{CR}=\text{CH}-\text{CH}=\text{CR}-$  or  $-\text{CH}=\text{CR}-\text{CR}=\text{CH}-$  linkage. The obtained **5b** has a  $-\text{CR}=\text{CH}-\text{CH}=\text{CR}-$  linkage formed via one of the head-to-head insertion mode. There is no evidence for other isomers. Similarly, although there are two possible regioisomers for the mononuclear complex **6**, only complexes having a  $-\text{CH}=\text{CR}(\text{O})\text{PPh}_2-$  linkage were obtained. All products **4**, **5**, and **6** are fairly stable in solution compared with **1**.



Dark brown crystals of **4c** suitable for X-ray crystal structure analysis were obtained by layering a toluene solution of **4c** with hexane at room temperature. Crystal data and structure refinement information of **4c** are presented in Table 1. The ORTEP drawing of **4c** is illustrated in Fig. 2 and selected bond distances and bond angles are given in Table 4. The X-ray structure analysis clearly shows that **4c** has a bridging phosphinoketoalkenyl ligand  $[\mu\text{-CH}=\text{CPhC}(\text{O})\text{PPh}_2]$  and a semi-bridging carbonyl ligand. The new ligand is coordinated to the Fe(1) atom by a phosphorus atom and the alkenyl carbon atom C(30) to make a five-membered  $\text{Fe}(1)\text{-P-C}(35)\text{-C}(29)\text{-C}(30)$  chelate ring. The double bond  $[\text{C}(29)\text{-C}(30)$  bond] of the chelate ring is bound to the Fe(2) atom in an  $\eta^2$ -fashion. The coordinated  $\text{C}(29)\text{-C}(30)$  bond length (1.433(17) Å) is typical for olefin-metal complexes with relatively strong back-donation [19]. The  $\text{P-C}(35)\text{-C}(29)\text{-C}(30)$  moiety is almost planar. The Fe(1) atom is slightly out of this plane. The geometry around the Fe(1) atom can be regarded as a distorted four-legged piano-stool when a metal-metal bond is included as one of four legs. The Fe(2) has bonding contacts with seven atoms and the geometry is close to a capped octahedron. The Fe-Fe bond length (2.636(3) Å) is comparable with that (av. 2.643(2) Å) found in the parent complex **1**. The Fe(1)-C(30) bond length (1.926(11) Å) is considerably shorter than those of Fe(2)-C bonds involving  $\pi$ -bonded carbon atoms

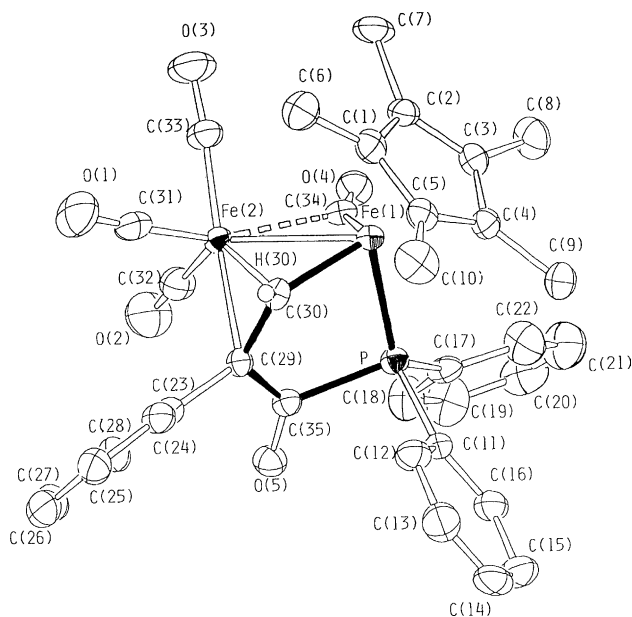


Fig. 2. ORTEP drawing of  $(\eta^5\text{-C}_5\text{Me}_5)\text{Fe}_2(\text{CO})_3(\mu\text{-CO})[\mu\text{-CH}=\text{CPhC}(\text{O})\text{PPh}_2] \cdot 3/2\text{C}_6\text{H}_5\text{CH}_3$  (**4c**:  $3/2\text{C}_6\text{H}_5\text{CH}_3$ ), showing 50% thermal ellipsoids. Hydrogen atoms except H(30) were omitted for clarity.

Table 4

Selected bond distances (Å) and angles (°) for  $(\eta^5\text{-C}_5\text{Me}_5)\text{Fe}_2(\text{CO})_3(\mu\text{-CO})[\mu\text{-CH}=\text{CPhC}(\text{O})\text{PPh}_2] \cdot 3/2\text{C}_6\text{H}_5\text{CH}_3$  (**4c**:  $3/2\text{C}_6\text{H}_5\text{CH}_3$ )

Bond distances			
Fe(1)–Fe(2)	2.636(3)	Fe(1)–P	2.181(3)
Fe(1)–C(30)	1.926(11)	Fe(2)–C(29)	2.158(8)
Fe(2)–C(30)	1.997(12)	Fe(1)–C(34)	1.793(11)
Fe(2)–C(34)	2.259(11)	C(29)–C(30)	1.433(17)
C(29)–C(35)	1.443(12)	P–C(35)	1.894(15)
Bond angles			
Fe(2)–Fe(1)–P	123.1(1)	Fe(1)–Fe(2)–C(30)	46.7(3)
Fe(1)–C(30)–Fe(2)	84.4(3)	Fe(2)–Fe(1)–C(30)	49.0(3)
Fe(1)–Fe(2)–C(29)	75.5(2)	Fe(1)–P–C(35)	101.6(5)
P–C(35)–C(29)	106.3(9)		

[Fe(2)–C(29) 2.158(8) Å, Fe(2)–C(30) 1.997(12) Å], reflecting the  $\sigma$ -bond character of the Fe(1)–C(30) bond. The existence of semi-bridging carbonyl ligand is demonstrated by the large difference between two Fe–C–O bond angles [153.1(12)°, 126.2(10)°] and two Fe–CO bond distances [1.739(11) Å, 2.259(11) Å] for the bridging carbonyl group.

According to the literature [20], a semi-bridging structure of a carbonyl ligand is often observed for multinuclear complexes in which the electron richness of metal atoms are not equal or the metal atoms are in sterically crowded situation. As there is no close contact between the bridging carbonyl ligand and the other ligands on two metals in **4c**, the net difference of electron richness between two metals in **4** must cause the semi-bridging structure. Since the oxidation numbers are 0 for Fe(2) and +2 for Fe(1), the Fe(2) atom could be

more electron rich than the Fe(1) atom and would tend to reduce the electron density by donating it from a filled  $d\pi$  orbital of the Fe(2) atom to the  $\pi^*$  orbital of the CO group attached to the Fe(1) atom. As a result, the bridging carbonyl ligand adopts a semi-bridging geometry. Another explanation would stem from a possible dative bond character of the metal–metal bond in **4c**. This is closely related to the explanation for the semi-bridging structure of one of the carbonyl ligands in  $\text{Fe}_2(\text{CO})_5(\mu\text{-CO})[\mu\text{-CMe}=\text{CMe}=\text{CMe}=\text{CMe}]$  [21]. Thus, we can count 18 electrons for the Fe(1) atom and 16 electrons for the Fe(2) atom when we ignore the metal–metal bond and the semi-bridging interaction between the Fe(2) atom and the carbonyl C(34)–O(4). In order to attain an 18-electron valence shell for each metal atom, the Fe–Fe bond must be considered as a dative bond from Fe(1) to Fe(2). The semi-bridging structure might serve to mitigate the resulting charge separation by the electron donation from Fe(2) to the  $\pi^*$  orbital of the CO group.

The spectral data of **4c** indicate that the crystal structure of **4c** is maintained in solution. Characteristic spectral features for **4c** are as follows: The  $^1\text{H}$  NMR signal of the  $\mu\text{-CH}$  in **4c** appears at 10.81 ppm as a doublet with a coupling constant  $^3J_{\text{PH}} = 2.0$  Hz. This low-field shift is attributable to the bridging-carbene-like situation of the methylene moiety, and is comparable to those of the  $\mu\text{-CH}$  in the complexes having an analogous five-membered metallacyclic ring, e.g.  $\text{RuCo}[\mu\text{-CH}=\text{C}(\text{SiMe}_3)\text{C}(\text{O})\text{PPh}_2](\mu\text{-CO})(\text{CO})_5$  (8.65 ppm, d,  $^3J_{\text{PH}} = 1.3$  Hz) [7]. The  $\mu\text{-CH}$  carbon signal appears at 168.1 ppm (d,  $^2J_{\text{PC}} = 21.1$  Hz), which is a typical chemical shift for a bridging carbene carbon. The  $^{13}\text{C}$  signals at 81.7 ppm (d,  $^2J_{\text{PC}} = 77.7$  Hz) and 199.7 ppm (d,  $^2J_{\text{PC}} = 38.3$  Hz) are assigned to the carbons for CPh moiety and the inserted carbonyl group [ $\text{—C}(\text{O})\text{PPh}_2$ ], respectively. A sharp singlet at 213.7 ppm suggests that the three terminal carbonyl ligands are mutually exchanging rapidly. A low-field resonance at 239.2 ppm (d,  $^2J_{\text{PC}} = 25.9$  Hz) is corresponding to the carbon of the semi-bridging carbonyl ligand. In the IR spectrum, broad CO stretching bands at 1857 and 1589  $\text{cm}^{-1}$  are assigned to the semi-bridging carbonyl and an inserted carbonyl in the  $[\mu\text{-CH}=\text{CPhC}(\text{O})\text{PPh}_2]$  ligand, respectively. The position of the latter is comparable with the corresponding bands (1600–1625  $\text{cm}^{-1}$ ) for the related complexes, e.g.,  $\text{RuCo}[\mu\text{-CR}^1=\text{CR}^2\text{C}(\text{O})\text{PPh}_2](\mu\text{-CO})(\text{CO})_5$  ( $\text{R}^1, \text{R}^2 = \text{Ph, Ph; Ph, H; }^t\text{Bu, H; H, SiMe}_3$ , etc.) [7]. Other spectral data of **4c** are consistent with the X-ray structure shown in Fig. 2. The spectral data of **4b** suggests that **4b** has a structure analogous to **4c** except for the reverse orientation of the inserted alkyne. The signal of the CH proton in the  $[\mu\text{-C}(\text{CO}_2\text{Me})=\text{CHC}(\text{O})\text{PPh}_2]$  ligand in **4b** was observed at 4.18 ppm, which is much higher in field compared with that (10.81 ppm) of **4c**, with a large coupling constant

$^3J_{\text{PH}} = 34.7$  Hz. This strongly suggests that **4b** differs from **4c** in the orientation of the inserted alkyne. The structure of **4a** was also determined as shown in Eq. (3) on the basis of the close similarities of spectral data among **4a**, **4b**, and **4c**.

Violet crystals of **5b** were obtained by layering a  $\text{CH}_2\text{Cl}_2$  solution of **5b** with hexane at room temperature and used for the X-ray crystal structure analysis. Crystal data and structure refinement information of **5b** are presented in Table 1. The ORTEP drawing of **5b** is illustrated in Fig. 3 and selected bond distances and bond angles are given in Table 5. Fig. 3 clearly shows that two iron atoms in **5b** are bridged by a new chelate ligand [ $\mu$ -

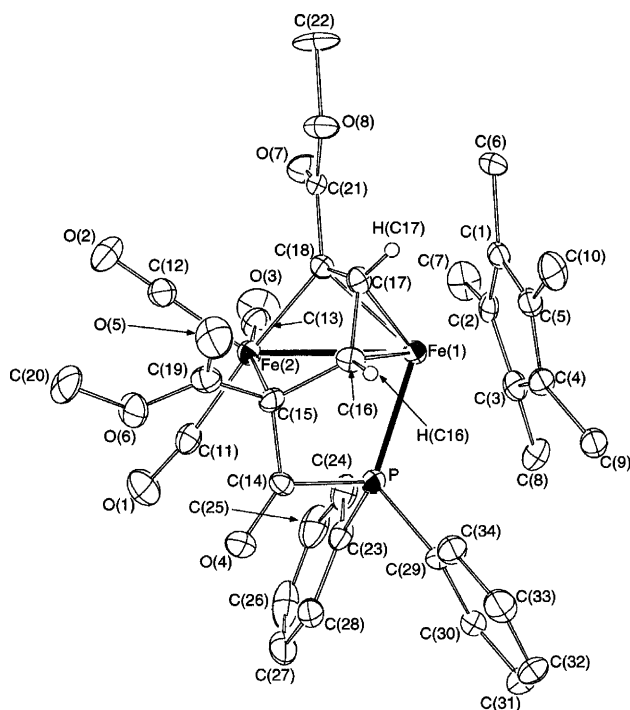


Fig. 3. ORTEP drawing of  $(\eta^5\text{-C}_5\text{Me}_5)\text{Fe}_2(\text{CO})_3[\mu\text{-CO}][\mu\text{-C}(\text{CO}_2\text{Me})\text{CHCHC}(\text{CO}_2\text{Me})\text{C}(\text{O})\text{PPh}_2]$  (**5b**), showing 50% thermal ellipsoids. Hydrogen atoms except H(C16) and H(C17) were omitted for clarity.

Table 5

Selected bond distances (Å) and angles (°) for  $(\eta^5\text{-C}_5\text{Me}_5)\text{Fe}_2(\text{CO})_3[\mu\text{-CO}][\mu\text{-C}(\text{CO}_2\text{Me})\text{CHCHC}(\text{CO}_2\text{Me})\text{C}(\text{O})\text{PPh}_2]$  (**5b**)

Bond distances			
Fe(1)–Fe(2)	2.759(2)	Fe(1)–P	2.242(2)
Fe(2)···P	2.985(3)	Fe(1)–C(16)	2.152(11)
Fe(1)–C(17)	2.065(12)	Fe(1)–C(18)	2.083(10)
Fe(2)–C(15)	2.163(9)	Fe(2)–C(18)	1.948(8)
P–C(14)	1.894(15)	C(14)–C(15)	1.461(13)
C(15)–C(16)	1.498(12)	C(16)–C(17)	1.388(12)
C(17)–C(18)	1.413(11)	C(14)–O(4)	1.225(10)
Bond angles			
Fe(2)–Fe(1)–P	72.46(7)	Fe(1)–Fe(2)–C(15)	59.6(3)
Fe(2)–Fe(1)–C(16)	69.6(3)	Fe(1)–Fe(2)–C(18)	93.0(3)
Fe(2)–Fe(1)–C(17)	70.7(3)	Fe(2)–Fe(1)–C(18)	44.8(3)
Fe(1)–C(18)–Fe(2)	86.3(4)	Fe(1)–P–C(14)	105.2(4)

$\text{C}(\text{CO}_2\text{Me})=\text{CH}-\text{CH}=\text{C}(\text{CO}_2\text{Me})\text{C}(\text{O})\text{PPh}_2]$  to form a seven-membered metallacyclic ring. Consequently, **5b** has a structure in which the second  $\text{MeO}_2\text{CC}\equiv\text{CH}$  is coupled with the  $\mu\text{-CH}$  carbon in a hypothetical regioisomer of **4c**,  $(\eta^5\text{-C}_5\text{Me}_5)\text{Fe}_2(\text{CO})_3[\mu\text{-CO}][\mu\text{-CH}=\text{C}(\text{CO}_2\text{Me})\text{C}(\text{O})\text{PPh}_2]$  (**4c'**), via head-to-head coupling. The Fe–Fe bond length (2.759(2) Å) is consistent with a single Fe–Fe bond, but significantly longer than those found in **1** (av. 2.643(2) Å) and **3a** (2.636(3) Å). The elongation of the Fe–Fe bond in **5b** may be explained by the dative bond character. According to the electron counting rule, the Fe(1) atom and the Fe(2) atom have 18 and 16 valence electrons, respectively, if the Fe–Fe bond is ignored: The new ligand is coordinated to the Fe(1) atom by the phosphorus atom and the C(16)–C(17)–C(18) moiety in a  $\pi$ -allyl fashion, and to the Fe(2) atom by two carbon atoms [C(15) and C(18)] in a  $\sigma$ -bonding fashion. Thus, to fulfill the 18 electron rule, the Fe(1) atom must donate two electrons to the Fe(2) atom. Then the oxidation numbers of both iron atoms in **5b** are +2. It should be noted that Mays et al. reported a dicobalt complex,  $\text{Co}_2(\text{CO})_4[\mu\text{-PPh}_2\text{CMe}=\text{CHC}(\text{O})\text{CH}=\text{CHPPh}_2]$ . The bridging ligand in this complex is similar to the bridging ligand in **5b** but is different in the linkage [5c].

The  $^1\text{H}$ ,  $^{13}\text{C}\{^1\text{H}\}$ ,  $^{13}\text{C}-^1\text{H}$  COSY,  $^{31}\text{P}$ , and IR spectra of **5b** are all consistent with the solid state structure. Some characteristic spectral features of **5b** can be summarized as follows. The two CH proton signals appear at 3.48 ppm (dd,  $^3J_{\text{HH}} = 4.0$  Hz,  $^3J_{\text{PH}} = 2.2$  Hz) and 6.20 ppm (dd,  $^3J_{\text{HH}} = 4.0$  Hz,  $^3J_{\text{PH}} = 1.6$  Hz) in the  $^1\text{H}$  NMR spectrum that can be assigned to coordinated olefin protons. Correspondingly, the two CH carbons appear at 62.8 ppm ( $J_{\text{PC}} = 5.0$  Hz) and 128.6 ppm ( $J_{\text{PC}} = 9.1$  Hz), respectively, which have been confirmed by the  $^{13}\text{C}-^1\text{H}$  COSY NMR spectroscopy. Three doublets at 75.8 ppm ( $^2J_{\text{PC}} = 86.3$  Hz), 171.9 ppm ( $^2J_{\text{PC}} = 34.7$  Hz), and 183.3 ppm ( $^1J_{\text{PC}} = 43.8$  Hz) in the  $^{13}\text{C}\{^1\text{H}\}$  NMR spectrum are assigned to the two carbons attached to  $\text{CO}_2\text{Me}$  groups, C(15) and C(18), and the inserted carbonyl carbon, C(14), respectively. The  $^{31}\text{P}$  NMR signal of **5b** appears at 75.9 ppm, which is comparable to those of **4a–c**. Similarly, based on the spectral data, complex **5a** is suggested to have a structure similar to **5b**.

The crystal structure of **6a** was determined as the representative of complexes **6a–c**. Orange plate-like crystals of **6a** were obtained by layering a toluene solution of **6a** with hexane at  $-30$  °C and used for the X-ray study. Crystal data and structure refinement information of **6a** are presented in Table 1. Two independent molecules (A and B) were found in the unit cell. As there is no significant difference between the two molecules, the ORTEP drawing of molecule A is illustrated in Fig. 4. Selected bond distances and bond angles for molecule A are given in Table 6. Fig. 4 clearly shows

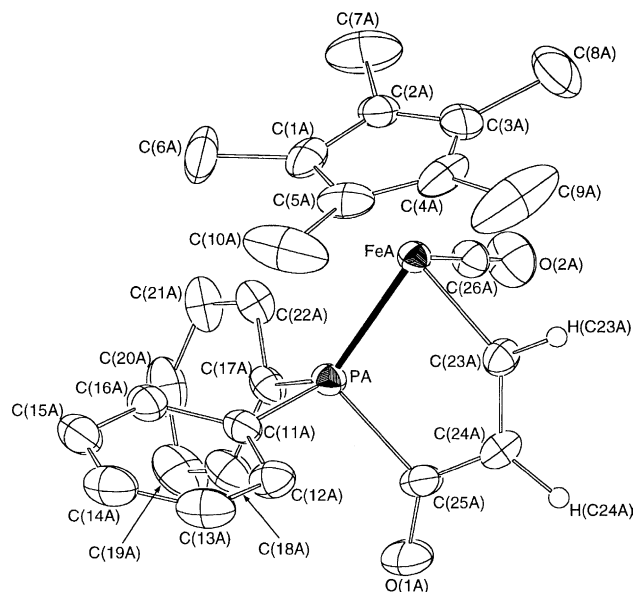


Fig. 4. ORTEP drawing of  $(\eta^5\text{-C}_5\text{Me}_5)\text{Fe}(\text{CO})[\text{CH}=\text{CHC}(\text{O})\text{PPh}_2]$  (**6a**), showing 50% thermal ellipsoids (Molecule A). Hydrogen atoms except H(C23A) and H(C24A) were omitted for clarity.

Table 6  
Selected bond distances (Å) and angles (°) for  $(\eta^5\text{-C}_5\text{Me}_5)\text{Fe}(\text{CO})[\text{CHCHC}(\text{O})\text{PPh}_2]$  (**6a**) (Molecule A)

Bond distances			
FeA–PA	2.180(2)	FeA–C(23A)	1.943(8)
C(23A)–C(24A)	1.355(12)	C(24A)–C(25A)	1.424(11)
C(25A)–O(1A)	1.219(11)	PA–C(25A)	1.917(9)
FeA–C(26A)	1.715(8)		
Bond angles			
PA–FeA–C(23A)	81.3(2)	PA–FeA–C(26A)	90.8(3)
C(23A)–FeA–C(26A)	87.3(3)	FeA–C(23A)–C(24A)	127.0(6)
C(23A)–C(24A)–C(25A)	117.3(7)	C(24A)–C(25A)–C(24A)	130.2(8)
PA–C(25A)–O(1A)	122.8(6)	FeA–PA–C(25A)	102.5(3)

that complex **6c** is a mononuclear complex having a chelate  $[\text{CH}=\text{CHC}(\text{O})\text{PPh}_2]$  ligand. The Fe atom adopts a three-legged piano-stool structure. The Fe–P distance (2.180(2) Å) is typical of the Fe–P dative bond. The C(23)–C(24) distance (1.355(12) Å) corresponds with a double bond. The Fe–C(23) distance (1.943(8) Å) is within a normal Fe–C  $\sigma$ -bond length.

There are some characteristic features in the spectral data of complex **6**. The proton of the Fe–CH= moiety shows a resonance at very low field (**6c**: 11.39 ppm, **6b**: 12.81 ppm, **6a**: 10.82 ppm) in the  $^1\text{H}$  NMR spectrum. This is surprising because the corresponding signals of the related complexes such as those of  $\alpha$ -CH of  $(\eta^5\text{-C}_5\text{Me}_5)\text{Fe}(\text{CO})_2(\eta^1\text{-CH}=\text{CH}_2)$  [22] and the  $\beta$ -CH of cyclopentenone [23] appear around 7–8 ppm. This anomaly can be rationalized by a large contribution of the canonical form **B** as a terminal carbene complex shown in Chart 3. The carbon signal for the Fe–CH= moiety of **6c**

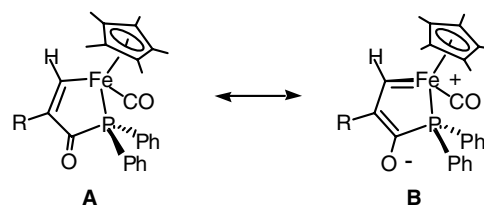
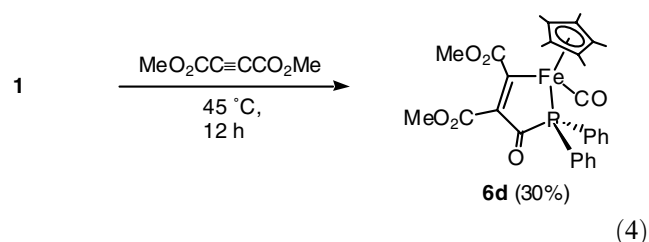


Chart 3.

also appears at very low field, 231.3 ppm ( $^2J_{\text{PC}} = 25.3$  Hz,  $^1J_{\text{CH}} = 136.6$  Hz), which is also in accord with the large contribution of form **B**. In addition, the carbon signals for the CPh= moiety, the C(O)P moiety, and a terminal carbonyl ligand of **6c** appear at 155.5 ppm ( $^2J_{\text{PC}} = 71.1$  Hz), 206.5 ppm ( $^2J_{\text{PC}} = 27.0$  Hz,  $^3J_{\text{CH}} = 15.6$  Hz), and 218.8 ppm ( $^2J_{\text{PC}} = 27.0$  Hz), respectively, which have been confirmed by the  $^{13}\text{C}$  NMR measurement in a  $^1\text{H}$  non-decoupling mode. The corresponding signals for complexes **6a** and **6b** appear in similar regions. There are some mononuclear complexes related to **6** but all of them have a ligand consisting of a carbonyl-alkene-phosphido linkage instead of an alkene-carbonyl-phosphido linkage: i.e.  $(\eta^5\text{-C}_5\text{H}_5)\text{Fe}(\text{CO})[\text{C}(\text{O})\text{CR}^1=\text{CR}^2\text{PPh}_2]$  ( $\text{R}^1 = \text{CO}_2\text{Me}$ ;  $\text{R}^2 = \text{H}$ ,  $\text{CO}_2\text{Me}$ ) [24] and  $(\eta^5\text{-C}_5\text{H}_5)\text{M}(\text{CO})_3\text{-}[\text{C}(\text{O})\text{CR}^1=\text{CR}^2\text{PPh}_2]$  ( $\text{M} = \text{Mo}$ ,  $\text{W}$ ;  $\text{R}^1 = \text{H}$ ,  $\text{R}^2 = \text{Ph}$ ,  $\text{CO}_2\text{Me}$ ;  $\text{R}^1 = \text{R}^2 = \text{CO}_2\text{Me}$ ,  $\text{CO}_2\text{Me}$ ) [25]. These complexes have been prepared by the reaction of the corresponding metallophosphines with alkynes.

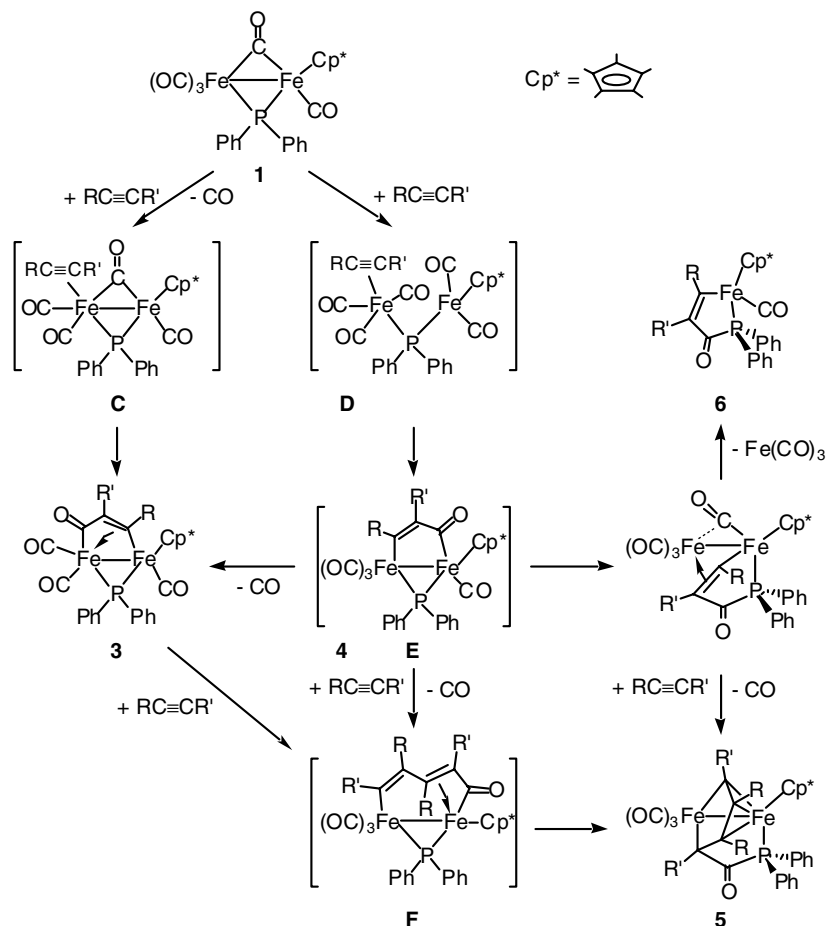
Although terminal alkynes easily reacted with **1** under mild conditions, inner alkynes such as diphenyl or di-*p*-tolyl acetylene did not react with **1** even at 80 °C. Only  $\text{MeO}_2\text{CC}\equiv\text{CCO}_2\text{Me}$  reacted with **1** to give a mononuclear iron complex  $(\eta^5\text{-C}_5\text{Me}_5)\text{Fe}(\text{CO})[\text{C}(\text{CO}_2\text{Me})=\text{C}(\text{CO}_2\text{Me})\text{C}(\text{O})\text{PPh}_2]$  (**6d**) as an isolable complex in 30% yield (Eq. (4)). The patterns of all NMR spectra of **6d** are very similar to those of **6a**, **6b**, and **6c**. The comparison of the carbon chemical shifts for the Fe–CR= moiety among complexes **6a–d** shows that **6d** has the strongest character of the above-mentioned terminal carbene complex (resonance form **B** in Chart 3): **6d** ( $\text{MeO}_2\text{CC}\equiv\text{CCO}_2\text{Me}$ ): 258.6 ppm, **6b** ( $\text{MeO}_2\text{CC}\equiv\text{CH}$ ): 253.3 ppm, **6c** ( $\text{PhC}\equiv\text{CH}$ ): 231.3 ppm, **6a** ( $\text{HC}\equiv\text{CH}$ ): 230.8 ppm. This is well explained by the electronic effect of the substituents on the inserted alkyne moiety: the strong electron-withdrawing group on the alkenyl moiety induces the strong  $\pi$ -back donation from the metal and results in giving the high double-bond character on the Fe–C carbon.



### 2.3. A plausible reaction mechanism

A plausible mechanism for the reaction of **1** with alkynes is illustrated in Scheme 2. The first step is most probably the coordination of the alkyne to the iron atom without a bulky  $\eta^5\text{-C}_5\text{Me}_5$  ligand with either metal–metal bond cleavage or CO loss to give intermediates **C** or **D**. Then, the coupling of a carbonyl group and the alkyne in **C** or **D** affords **3** or the intermediate **E**, respectively. An intermediate related to **E** involving a five-membered  $\text{M}-\text{CR}=\text{CR}'-\text{C}(\text{O})-\text{M}$  metallacyclic ring has been previously proposed in the reaction of  $\text{Co}_2(\mu\text{-HC}\equiv\text{CH})(\text{CO})_6$  with  $\text{P}_2\text{Ph}_4$  to give  $\text{Co}_2[\mu\text{-HX}=\text{CHC}(\text{O})\text{PPh}_2](\mu\text{-PPh}_2)(\text{CO})_4$  [26]. A CO loss from **E** leads to the formation of **3** in the case of  $\text{tBuC}\equiv\text{CH}$ . Without a CO loss, the insertion of the phosphido ligand into the  $\text{Fe}-\text{C}(\text{O})$  bond in **E** produces **4** in the case of  $\text{RC}\equiv\text{CR}'$  ( $\text{R}=\text{H}$ ,  $\text{R}'=\text{CO}_2\text{Me}$ ,  $\text{Ph}$ ). There are some examples for insertion of the phosphido ligand into the  $\text{M}-\text{C}(\text{O})\text{R}$  bond [27]. There are two paths to be considered for the formation of **5** from the proposed intermediate **E**. One is the path via **4**: an

insertion of another alkyne into a  $\text{C}-\text{Fe}$  bond of **4** accompanied by a CO dissociation gives **5**. The other path includes an initial insertion of another alkyne into a  $\text{C}-\text{Fe}$  bond of **E** accompanied by a CO dissociation to give intermediate **F**. Then, the insertion of the phosphido ligand into the  $\text{Fe}-\text{C}(\text{O})$  bond in **F** accompanied by rearrangement occurs to afford **5**. Intermediate **F** might also be formed from the reaction of **3** with an alkyne. Complex **5b** may be formed from a hypothetical regioisomer of **4b**,  $(\eta^5\text{-C}_5\text{Me}_5)\text{Fe}_2(\text{CO})_4[\mu\text{-CH}=\text{C}(\text{CO}_2\text{Me})\text{C}(\text{O})\text{PPh}_2]$  (**4b'**), and  $\text{MeO}_2\text{CC}\equiv\text{CH}$  via head-to-head coupling. The bridging moiety of **4b'** are less hindered and could react with another alkyne to produce **5b**. In fact, more hindered **4b** did not react with another molecule of  $\text{MeO}_2\text{CC}\equiv\text{CH}$ . We found that **4a** reacted with  $\text{HC}\equiv\text{CH}$ , but produced only a trace of **5a**. Therefore, this reaction may proceed mainly through **F**. Mononuclear complex **6** can form by the thermal decomposition of **4** with liberation of a  $\text{Fe}(\text{CO})_3$  fragment. This is consistent with the fact that prolonged heating of the solution of **4a** or **4c** leads to the principal formation of **6a** or **6c**, respectively

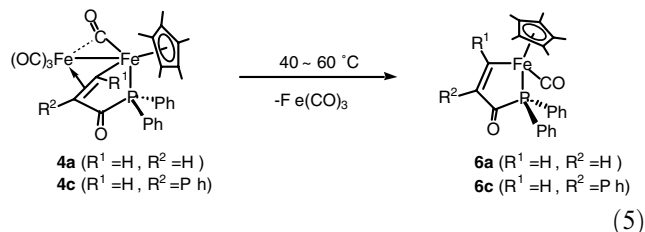


Scheme 2.

(Eq. (5)). The regiochemistry of the products **3–6** seems to be controlled at the step of the alkyne insertion (from **C** or **D** to **E**) by minimizing the steric interaction between the bulky  $\eta^5\text{-C}_5\text{Me}_5$  group on the other metal and the substituent on the alkyne, though electronic factors cannot be ignored.

#### 2.4. Summary

Complex  $(\eta^5\text{-C}_5\text{Me}_5)\text{Fe}_2(\text{CO})_4(\mu\text{-CO})(\mu\text{-PPh}_2)$  (**1**) was prepared in high yield by a new method, i.e., the coupling between the anionic phosphido iron complex  $\text{Li}[\text{Fe}(\text{CO})_4\text{PPh}_2]$  with  $(\eta^5\text{-C}_5\text{Me}_5)\text{Fe}(\text{CO})_2\text{I}$  followed by photolysis. The X-ray crystal structure analysis of **1** revealed that the two bridging ligands, phosphido and carbonyl, are both almost symmetrically coordinated to two metals, despite the differences in ligands and oxidation numbers between the two metal fragments. The large steric repulsion between a bulky  $\eta^5\text{-C}_5\text{Me}_5$  group and a phenyl group on the bridging phosphido ligand is notable. The reactions of **1** with various terminal alkynes produced complexes incorporating one or two molecules of alkynes and a carbonyl group as a result of C–C bond and P–C bond formation. The structures of three types of products except for **3** have been determined by X-ray crystal structure analysis. The reaction of **1** with  $^t\text{BuC}\equiv\text{CH}$ , a terminal alkyne with a bulky group, gave a mixture of two isomeric complexes  $(\eta^5\text{-C}_5\text{Me}_5)\text{Fe}_2(\text{CO})_3(\mu\text{-PPh}_2)(\mu\text{-CH}=\text{C}(^t\text{Bu})\text{C}(\text{O}))$  (**3**) containing a ketoalkenyl ligand [17]. For the terminal alkynes with a less hindered and/or electron-withdrawing group, the principal products were dinuclear complexes bridged by a new phosphinoketoalkenyl ligand,  $(\eta^5\text{-C}_5\text{Me}_5)\text{Fe}_2(\text{CO})_3(\mu\text{-CO})[\mu\text{-CR}^1=\text{CR}^2\text{C}(\text{O})\text{PPh}_2]$  (**4a**:  $\text{R}^1 = \text{H}$ ,  $\text{R}^2 = \text{H}$ ; **4b**:  $\text{R}^1 = \text{CO}_2\text{Me}$ ,  $\text{R}^2 = \text{H}$ ; **4c**:  $\text{R}^1 = \text{H}$ ,  $\text{R}^2 = \text{Ph}$ ). In the cases of alkynes  $\text{RC}\equiv\text{CH}$  ( $\text{R} = \text{CO}_2\text{Me}$ ,  $\text{H}$ ), double insertion of alkynes into a metal–phosphido bond accompanied by CO insertion also occurred to produce dinuclear complexes  $(\eta^5\text{-C}_5\text{Me}_5)\text{Fe}_2(\text{CO})_3[\mu\text{-CRCHCHCRC}(\text{O})\text{PPh}_2]$  (**5a**:  $\text{R} = \text{H}$ ; **5b**:  $\text{R} = \text{CO}_2\text{Me}$ ). In all cases, mononuclear complexes,  $(\eta^5\text{-C}_5\text{Me}_5)\text{Fe}(\text{CO})[\text{CR}^1 = \text{CR}^2\text{C}(\text{O})\text{PPh}_2]$  (**6a**:  $\text{R}^1 = \text{H}$ ,  $\text{R}^2 = \text{H}$ ; **6b**:  $\text{R}^1 = \text{H}$ ,  $\text{R}^2 = \text{CO}_2\text{Me}$ ; **6c**:  $\text{R}^1 = \text{H}$ ,  $\text{R}^2 = \text{Ph}$ ) were isolated in low yields. Most of inner alkynes did not react with **1** even at high temperatures, but highly electron deficient  $\text{MeO}_2\text{CC}\equiv\text{C-CO}_2\text{Me}$  reacted with **1** to give a mononuclear iron complex  $(\eta^5\text{-C}_5\text{Me}_5)\text{Fe}(\text{CO})[\text{C}(\text{CO}_2\text{Me})=\text{C}(\text{CO}_2\text{Me})\text{C}(\text{O})\text{PPh}_2]$  (**6d**) as only an isolable complex in low yield. According to the spectroscopic data, these dinuclear complexes have a nature of the carbene-bridged dinuclear complexes and mononuclear complexes have a strong character of the terminal carbene complex (canonical form **B** in Chart 3).



A plausible reaction mechanism for the formation of these products was suggested. The key steps are (1) initial coordination of an alkyne, (2) coupling of the coordinated alkyne with a carbonyl ligand, and (3) formation of an alkyne-carbonyl-phosphido linkage. The regiochemistry of the products **3–6** seems to be controlled mainly at the step after the coupling of the coordinated alkyne with a carbonyl ligand on a metal by minimizing the steric interaction between the bulky  $\eta^5\text{-C}_5\text{Me}_5$  group on the other metal and the substituent on the alkyne. When the substituent on a terminal alkyne is small or electron-withdrawing ( $\text{H}$ ,  $\text{CO}_2\text{Me}$ ), the second alkyne can insert into a C–Fe bond to produce dinuclear complexes having a  $[\mu\text{-CRCHCHCRC}(\text{O})\text{PPh}_2]$  ligand.

### 3. Experimental details

#### 3.1. General procedure

All manipulations were carried out under a dry nitrogen or argon atmosphere using standard Schlenk techniques. Hexane, benzene, toluene, ether, and THF were distilled from sodium/benzophenone before use.  $\text{Fe}(\text{CO})_4\text{PPh}_2\text{H}$  [28],  $(\eta^5\text{-C}_5\text{Me}_5)\text{Fe}(\text{CO})_2\text{I}$  [29],  $\text{PhC}\equiv\text{CH}$  [30], and  $^t\text{BuC}\equiv\text{CH}$  [31] were prepared according to the literature methods.  $\text{MeO}_2\text{CC}\equiv\text{CH}$  and  $\text{MeO}_2\text{CC}\equiv\text{CCO}_2\text{Me}$  were purchased and dried over molecular sieves 4A before use.  $^1\text{H}$  and  $^{13}\text{C}$  NMR spectra were recorded on Bruker ARX-300 and Varian XL-200 instruments.  $^{31}\text{P}$  NMR spectra were recorded on JEOL FX-90Q and Bruker ARX-300 spectrometers referenced to external 85%  $\text{H}_3\text{PO}_4$ . IR spectra were obtained with a Horiba FT-200 spectrophotometer, and mass spectra were obtained on Hitachi M-2500S and JEOL JMS HX-110 spectrometers. Irradiation was carried out using a 450-W medium-pressure Hg arc lamp (Ushio UV-450).

#### 3.2. Preparation of $(\eta^5\text{-C}_5\text{Me}_5)\text{Fe}_2(\text{CO})_4(\mu\text{-CO})(\mu\text{-PPh}_2)$ (**1**) (a new method)

To a solution of  $\text{Fe}(\text{CO})_4\text{PPh}_2\text{H}$  (1.00 g, 2.83 mmol) in THF (20 ml) was added 2.0 ml (3.4 mmol) of *n*-butyllithium (1.63 M in hexane) at 0 °C. The color of the

solution changed to dark red. A solution of ( $\eta^5$ -C<sub>5</sub>Me<sub>5</sub>)Fe(CO)<sub>2</sub>I (1.06 g, 2.82 mmol) in THF (20 ml) was added within 10 min to the above solution and the resulting solution was stirred overnight. After filtration of the reaction mixture with alumina (activated with a microwave oven for 3 minutes), removal of solvent from the filtrate under reduced pressure gave crude ( $\eta^5$ -C<sub>5</sub>Me<sub>5</sub>)Fe<sub>2</sub>(CO)<sub>6</sub>( $\mu$ -PPh<sub>2</sub>) (**2**) in 97% yield (1.65 g, 2.74 mmol). A benzene (280 ml) solution of **2** (0.610 g, 1.02 mmol) was irradiated with a 450-W medium-pressure Hg lamp for 7 h. After removal of the solvent under reduced pressure, the residue was chromatographed on an alumina column (300 mesh, i.d. 2.3 cm  $\times$  7 cm; eluent: hexane/benzene = 2/1). Concentration of a black fraction gave ( $\eta^5$ -C<sub>5</sub>Me<sub>5</sub>)Fe<sub>2</sub>(CO)<sub>4</sub>( $\mu$ -CO)( $\mu$ -PPh<sub>2</sub>) (**1**) in 76% yield (0.446 g, 0.779 mmol). **2**: <sup>1</sup>H NMR (300 MHz, C<sub>6</sub>D<sub>6</sub>)  $\delta$  1.39 (s, 15H, Me), 6.8–8.4 (m, 10H, Ph), <sup>31</sup>P NMR (36.3 MHz, C<sub>6</sub>D<sub>6</sub>)  $\delta$  90.8. IR (KBr)  $\nu_{\text{CO}}$  1998 (vs), 1948 (vs), 1930 (sh, vs), 1871 (s), 1851 (vs), 1840 (vs) cm<sup>-1</sup>.

### 3.3. Reaction of ( $\eta^5$ -C<sub>5</sub>Me<sub>5</sub>)Fe<sub>2</sub>(CO)<sub>4</sub>( $\mu$ -CO)( $\mu$ -PPh<sub>2</sub>) (**1**) with <sup>t</sup>BuC $\equiv$ CH

A solution of **1** (400 mg, 0.699 mmol) and <sup>t</sup>BuC $\equiv$ CH (GC 86% pure, 100 mg, 1.05 mmol) in benzene (20 ml) was stirred for 40 h at 35 °C. After removal of solvent, the residue was chromatographed on a silica gel flash column (silica gel 35 g, 1.8  $\times$  16 cm). Elution with CH<sub>2</sub>Cl<sub>2</sub>/hexane (5/1) gave a brown fraction, which contained several unidentified products, and a dark green fraction. The eluent was then changed to CH<sub>2</sub>Cl<sub>2</sub> to collect a brown fraction. The color of both dark green and brown fractions changed to greenish brown even during elution. Concentration of each of the last two fractions afforded the same isomeric mixture of ( $\eta^5$ -C<sub>5</sub>Me<sub>5</sub>)Fe<sub>2</sub>(CO)<sub>3</sub>( $\mu$ -PPh<sub>2</sub>)[ $\mu$ -CH=C(<sup>t</sup>Bu)C(O)] (**3a** and **3b**) in 59% total yield (259 mg, 0.414 mmol). The <sup>1</sup>H and <sup>31</sup>P NMR, and IR spectral data for a mixture of **3a** and **3b** are listed in Table 3. **3a** and **3b**: <sup>13</sup>C NMR (75.5 MHz, C<sub>6</sub>D<sub>6</sub>)  $\delta$  9.4 (C<sub>5</sub>Me<sub>5</sub>), 9.9 (C<sub>5</sub>Me<sub>5</sub>), 28.8 (CMe<sub>3</sub>), 29.2 (CMe<sub>3</sub>), 33.2 (d, <sup>4</sup>J<sub>PC</sub> = 0.9 Hz, CMe<sub>3</sub>), 34.0 (d, <sup>4</sup>J<sub>PC</sub> = 0.8 Hz, CMe<sub>3</sub>), 70.8 (d, <sup>3</sup>J<sub>PC</sub> = 2.6 Hz, CBu<sup>t</sup>), 77.8 (d, <sup>3</sup>J<sub>PC</sub> = 2.6 Hz, CBu<sup>t</sup>), 96.5 (C<sub>5</sub>Me<sub>5</sub>), 97.3 (C<sub>5</sub>Me<sub>5</sub>), 129.15 (d, J<sub>PC</sub> = 2.1 Hz, PPh<sub>2</sub>), 129.24 (d, J<sub>PC</sub> = 2.1 Hz, PPh<sub>2</sub>), 129.5 (d, J<sub>PC</sub> = 3.4 Hz, PPh<sub>2</sub>), 130.2 (d, J<sub>PC</sub> = 3.4 Hz, PPh<sub>2</sub>), 133.3 (d, J<sub>PC</sub> = 8.3 Hz, PPh<sub>2</sub>), 134.5, 134.63, 134.66, 134.8, 135.3, 135.5 (PPh<sub>2</sub>), 139.8 (d, J<sub>PC</sub> = 43 Hz, PPh<sub>2</sub>), 142.3 (d, J<sub>PC</sub> = 18 Hz, PPh<sub>2</sub>), 143.3 (d, J<sub>PC</sub> = 26 Hz, PPh<sub>2</sub>), 144.9 (d, J<sub>PC</sub> = 36 Hz, PPh<sub>2</sub>), 185.1 (d, <sup>2</sup>J<sub>PC</sub> = 4.2 Hz, CH), 189.3 (d, <sup>2</sup>J<sub>PC</sub> = 3.4 Hz, CH), 209.7 (d, <sup>2</sup>J<sub>PC</sub> = 1.3 Hz, CO), 212.2 (d, <sup>2</sup>J<sub>PC</sub> = 3.9 Hz, CO), 213.9 (d, <sup>2</sup>J<sub>PC</sub> = 14 Hz, CO), 214.3 (d, <sup>2</sup>J<sub>PC</sub> = 17 Hz, CO), 220.5 (d, <sup>2</sup>J<sub>PC</sub> = 11 Hz, CO), 221.0 (d, <sup>2</sup>J<sub>PC</sub> = 10 Hz, CO), 227.8 (d, <sup>2</sup>J<sub>PC</sub> = 8.5 Hz, CO), 228.1 (d, <sup>2</sup>J<sub>PC</sub> = 12 Hz, CO). Mass (FAB, Xe,

*m*-nitrobenzyl alcohol matrix) *m/z* 627 (M<sup>+</sup> + 1, 54.4), 598 (M<sup>+</sup> - CO, 10.5), 570 (M<sup>+</sup> - 2CO, 100), 542 (M<sup>+</sup> - 3CO, 58.3), 514 (M<sup>+</sup> - 4CO, 70.7), 376 ((C<sub>5</sub>Me<sub>5</sub>)Fe-PPh<sub>2</sub>, 88.5). Exact mass calcd for C<sub>32</sub>H<sub>35</sub>Fe<sub>2</sub>O<sub>4</sub>P: 626.0972. Found: 626.0974.

### 3.4. Reaction of ( $\eta^5$ -C<sub>5</sub>Me<sub>5</sub>)Fe<sub>2</sub>(CO)<sub>4</sub>( $\mu$ -CO)( $\mu$ -PPh<sub>2</sub>) (**1**) with HC $\equiv$ CH

Acetylene gas was bubbled through a solution of **1** (100 mg, 0.175 mmol) in benzene (20 ml) for 3 h at 40 °C. After removal of volatiles, the residue was chromatographed on a silica gel flash column (silica gel 30 g, 1.5  $\times$  18 cm). Elution with CH<sub>2</sub>Cl<sub>2</sub>/hexane (3/1) gave unidentified brown products, orange crystals of ( $\eta^5$ -C<sub>5</sub>Me<sub>5</sub>)Fe(CO)[CH=CHC(O)PPh<sub>2</sub>] (**6a**) in 24% yield (19 mg, 0.041 mmol), and then brown crystals of ( $\eta^5$ -C<sub>5</sub>Me<sub>5</sub>)Fe<sub>2</sub>(CO)<sub>3</sub>[ $\mu$ -CHCHCHC(O)PPh<sub>2</sub>] (**5a**) in 7% yield (7 mg, 0.01 mmol). Finally elution with CH<sub>2</sub>Cl<sub>2</sub> gave olive crystals of ( $\eta^5$ -C<sub>5</sub>Me<sub>5</sub>)Fe<sub>2</sub>(CO)<sub>3</sub>( $\mu$ -CO)[ $\mu$ -CH=CHC(O)PPh<sub>2</sub>] (**4a**) in 24% yield (18 mg, 0.030 mmol). The <sup>1</sup>H and <sup>31</sup>P NMR, and IR spectral data for **4a**, **5a**, and **6a** are listed in Table 3. **4a**: <sup>13</sup>C NMR (75.5 MHz, C<sub>6</sub>D<sub>6</sub>)  $\delta$  9.1 (C<sub>5</sub>Me<sub>5</sub>), 66.2 (d, <sup>2</sup>J<sub>PC</sub> = 82.6 Hz, -C HC(O)-), 85.9 (d, <sup>3</sup>J<sub>PC</sub> = 0.9 Hz, C<sub>5</sub>Me<sub>5</sub>), 127-129 (m, PPh<sub>2</sub>), 130.1 (d, J<sub>PC</sub> = 2.9 Hz, PPh<sub>2</sub>), 131.0 (d, J<sub>PC</sub> = 2.3 Hz, PPh<sub>2</sub>), 132.75 (d, J<sub>PC</sub> = 9.0 Hz, PPh<sub>2</sub>), 132.81 (d, J<sub>PC</sub> = 39.5 Hz, PPh<sub>2</sub>), 134.3 (d, J<sub>PC</sub> = 7.6 Hz, PPh<sub>2</sub>), 168.9 (d, <sup>2</sup>J<sub>PC</sub> = 19.7 Hz,  $\mu$ -CH), 206.7 (d, <sup>1</sup>J<sub>PC</sub> = 31.9 Hz, -C(O)PPh<sub>2</sub>-), 213.9 (s, CO), 239.6 (d, <sup>2</sup>J<sub>PC</sub> = 26.2 Hz,  $\mu$ -CO). Mass (FAB, Xe, *m*-nitrobenzyl alcohol matrix) *m/z* 599 (M<sup>+</sup>+1, 32.4), 571 (M<sup>+</sup> - CO+1, 9.6), 542 (M<sup>+</sup> - 2CO, 68.3), 514 (M<sup>+</sup> - 3CO, 100), 486 (M<sup>+</sup> - 4CO, 53.5), 458 (M<sup>+</sup> - 5CO, 65.2), 402 (M<sup>+</sup> - 5CO-Fe, 66.9), 376 ((C<sub>5</sub>Me<sub>5</sub>)FePPh<sub>2</sub>, 97.0). Anal. Calcd for C<sub>29</sub>H<sub>27</sub>Fe<sub>2</sub>O<sub>5</sub>P: C, 58.23; H, 4.55. Found: C, 58.05; H, 4.70. **5a**: <sup>13</sup>C NMR (75.5 MHz, C<sub>6</sub>D<sub>6</sub>)  $\delta$  9.1 (C<sub>5</sub>Me<sub>5</sub>), 67.3 (d, <sup>2</sup>J<sub>PC</sub> = 59.2 Hz, =CHC(O)-), 87.3 (C<sub>5</sub>Me<sub>5</sub>), 89.0 (d, <sup>2</sup>J<sub>PC</sub> = 3.3 Hz, CH), 110.2 (d, <sup>2</sup>J<sub>PC</sub> = 10.2 Hz, CH), 127-129 (PPh<sub>2</sub>), 129.9 (d, J<sub>PC</sub> = 2.7 Hz, PPh<sub>2</sub>), 130.0 (d, J<sub>PC</sub> = 2.6 Hz, PPh<sub>2</sub>), 133.9 (d, J<sub>PC</sub> = 7.7 Hz, PPh<sub>2</sub>), 134.5 (d, J<sub>PC</sub> = 8.6 Hz, PPh<sub>2</sub>), 130-134 (m, PPh<sub>2</sub>), 161.5 (d, <sup>2</sup>J<sub>PC</sub> = 24.5 Hz,  $\mu$ -CH), 190.3 (d, <sup>2</sup>J<sub>PC</sub> = 18.1 Hz, -C(O)PPh<sub>2</sub>-). Mass (FAB, Xe, *m*-nitrobenzyl alcohol matrix) *m/z* 597 (M<sup>+</sup>+1, 2.3), 568 (M<sup>+</sup>-CO, 14.0), 540 (M<sup>+</sup>-2CO, 9.3), 512 (M<sup>+</sup>-3CO, 54.0), 484 (M<sup>+</sup>-4CO, 100). **6a**: <sup>13</sup>C NMR (75.5 MHz, C<sub>6</sub>D<sub>6</sub>,  $\delta$ ) 9.6 (C<sub>5</sub>Me<sub>5</sub>), 93.3 (C<sub>5</sub>Me<sub>5</sub>), 127-129 (PPh<sub>2</sub>), 129.5 (d, J<sub>PC</sub> = 2.3 Hz, PPh<sub>2</sub>), 130.9 (d, J<sub>PC</sub> = 2.3 Hz, PPh<sub>2</sub>), 131.2 (d, J<sub>PC</sub> = 32.5 Hz, PPh<sub>2</sub>), 132.6 (d, J<sub>PC</sub> = 9.1 Hz, PPh<sub>2</sub>), 135.5 (d, J<sub>PC</sub> = 28.7 Hz, PPh<sub>2</sub>), 136.0 (d, J<sub>PC</sub> = 9.8 Hz, PPh<sub>2</sub>), 146.0 (ddd (<sup>1</sup>H nondecoupling mode), <sup>2</sup>J<sub>PC</sub> = 74.7 Hz, <sup>1</sup>J<sub>CH</sub> = 160.9 Hz, <sup>3</sup>J<sub>CH</sub> = 1.7 Hz, =CHC(O)-), 209.3 (d, <sup>1</sup>J<sub>PC</sub> = 26.3 Hz, -C(O)PPh<sub>2</sub>), 219.4 (d, <sup>2</sup>J<sub>PC</sub> = 26.8 Hz, CO), 230.8 (dd, <sup>2</sup>J<sub>PC</sub> = 22.3 Hz, <sup>1</sup>J<sub>CH</sub> = 139.3 Hz, Fe-CH=). Mass

(FAB, Xe, *m*-nitrobenzyl alcohol matrix) *m/z* 459 ( $M^+ + 1$ , 54.3), 431 ( $M^+ - CO + 1$ , 32.2), 402 ( $M^+ - 2CO$ , 91.9), 376 ( $(C_5Me_5)FePPh_2$ , 100). Exact mass calcd for  $C_{26}H_{27}FeO_2P$ : 458.1098. Found: 458.1098.

### 3.5. Reaction of $(\eta^5-C_5Me_5)Fe_2(CO)_4(\mu-CO)(\mu-PPh_2)$ (**1**) with $MeO_2CC\equiv CH$

A solution of **1** (252 mg, 0.440 mmol) and  $MeO_2CC\equiv CH$  (55 mg, 0.66 mmol) in benzene (15 ml) was stirred for 20 h at 40 °C. After removal of solvent, the residue was dissolved in a minimum amount of  $CH_2Cl_2$ , absorbed with Celite, and solvent removed, and the remaining Celite with the sample was placed on the top of a column (silica gel 35 g,  $2.3 \times 9$  cm). The first brown fraction was eluted with  $CH_2Cl_2$ /ether (5 / 1), which contained some products. The second fraction was eluted with ether and removal of solvent gave violet crystals of  $(\eta^5-C_5Me_5)Fe_2(CO)_3[\mu-C(CO_2Me)CHCHC(CO_2Me)C(O)PPh_2]$  (**5b**) (89 mg). The first brown fraction was chromatographed again on alumina (300 mech,  $1.5 \times 10$  cm) and elution with  $CH_2Cl_2$ /ether (1/1) gave  $(\eta^5-C_5Me_5)Fe_2(CO)_3(\mu-CO)[\mu-C(CO_2Me)=CHC(O)PPh_2]$  (**4b**) as a dark brown solid in 54% yield (119 mg, 0.240 mmol) and  $(\eta^5-C_5Me_5)Fe(CO)[CH=C(CO_2Me)C(O)PPh_2]$  (**6b**) as an orange solid in 2% yield (4.0 mg, 0.008 mmol). Finally, another 30 mg of **5b** was obtained from the eluate with EtOH. The total yield of **5b** was 38% (119 mg, 0.167 mmol). The  $^1H$  and  $^{31}P$  NMR, and IR spectral data for **4b**, **5b**, and **6b** are listed in Table 3. **4b**:  $^{13}C$  NMR (75.5 MHz,  $C_6D_6$ )  $\delta$  8.7 ( $C_5Me_5$ ), 51.6 ( $CO_2Me$ ), 73.8 (d,  $J_{PC} = 82.8$  Hz, CH), 95.2 ( $C_5Me_5$ ), 128.4 (d,  $J_{PC} = 6.8$  Hz, PPh<sub>2</sub>), 128.7 (d,  $J_{PC} = 9.8$  Hz, PPh<sub>2</sub>), 130.3 (d,  $J_{PC} = 2.8$  Hz, PPh<sub>2</sub>), 130.9 (d,  $J_{PC} = 2.7$  Hz, PPh<sub>2</sub>), 131.7 (d,  $J_{PC} = 8.3$  Hz, PPh<sub>2</sub>), 134.9 (d,  $J_{PC} = 6.8$  Hz, PPh<sub>2</sub>), 134.9 (d,  $J_{PC} = 36.0$  Hz, PPh<sub>2</sub>), 145.8 (d,  $^3J_{PC} = 17.3$  Hz,  $CCO_2Me$ ), 178.8 ( $CO_2Me$ ), 200.3 (d,  $^1J_{PC} = 25.5$  Hz,  $-C(O)PPh_2-$ ), 211 (br, CO), 230.5 (CO). Mass (FAB, Xe, *m*-nitrobenzyl alcohol matrix) *m/z* 657 ( $M^+ + 1$ , 100.0), 628 ( $M^+ - CO$ , 15.0), 600 ( $M^+ - 2CO$ , 10.5), 572 ( $M^+ - 3CO$ , 59.9), 544 ( $M^+ - 4CO$  or  $M^+ - HCCCO_2Me$ , 89.5), 516 ( $M^+ - 5CO$  or  $M^+ - CO - HCCCO_2Me$ , 38.0). 488 ( $M^+ - 2CO - HCCCO_2Me$ , 63.3). Anal. Calcd for  $C_{31}H_{29}Fe_2O_7P$ : C, 56.74; H, 4.45. Found: C, 57.01; H, 4.53. **5b**:  $^{13}C$  NMR (50 MHz,  $CD_2Cl_2$ ,  $\delta$ ) 9.4 ( $C_5Me_5$ ), 50.9 ( $CO_2Me$ ), 51.9 ( $CO_2Me$ ), 62.8 (d,  $^2J_{PC} = 7.5$  Hz, CH), 75.8 (d,  $^2J_{PC} = 86.3$  Hz,  $=C(CO_2Me)C(O)-$ ), 93.4 ( $C_5Me_5$ ), 103.7 (CH), 128.6 (d,  $J_{PC} = 9.1$  Hz, PPh<sub>2</sub>), 130.3 (d,  $J_{PC} = 2.3$  Hz, PPh<sub>2</sub>), 130.6 (d,  $J_{PC} = 3.0$  Hz, PPh<sub>2</sub>), 134.6 (d,  $J_{PC} = 8.3$  Hz, PPh<sub>2</sub>), 136.8 (d,  $J_{PC} = 9.1$  Hz, PPh<sub>2</sub>), 137.0 (d,  $J_{PC} = 25.7$  Hz, PPh<sub>2</sub>), 138.4 (d,  $J_{PC} = 43.0$  Hz, PPh<sub>2</sub>), 160.2 ( $CO_2Me$ ), 171.9 (d,  $^2J_{PC} = 34.7$  Hz,  $\mu-C(CO_2Me)=$ ), 178.2 ( $CO_2Me$ ), 183.3 (d,  $^2J_{PC} = 43.8$  Hz,  $-C(O)PPh_2-$ ), 207.3 (d,  $^3J_{PC} = 5.5$  Hz, CO), 210.5 (d,  $^3J_{PC} = 1.7$  Hz, CO), 210.8 (d,

$^3J_{PC} = 3.9$  Hz, CO). Mass (FAB, Xe, *m*-nitrobenzyl alcohol matrix) *m/z* 713 ( $M^+ + 1$ , 12.7), 628 ( $M^+ - HCCCO_2Me$ , 22.6), 392 ( $Fe_2(CO)_4(HCCCO_2Me)$ , 100). Anal. Calcd for  $C_{34}H_{33}Fe_2O_8P$ : C, 57.33; H, 4.67. Found: C, 57.03; H, 4.80. **6b**:  $^{13}C$  NMR (75.5 MHz,  $C_6D_6$ )  $\delta$  9.5 ( $C_5Me_5$ ), 50.8 ( $CO_2Me$ ), 94.7 ( $C_5Me_5$ ), 127.3 (PPh<sub>2</sub>), 127.3 (PPh<sub>2</sub>), 129.9 (d,  $J_{PC} = 2.3$  Hz, PPh<sub>2</sub>), 130.4, 130.9 (PPh<sub>2</sub>), 131.2 (d,  $J_{PC} = 2.3$  Hz, PPh<sub>2</sub>), 132.3 (d,  $J_{PC} = 8.3$  Hz, PPh<sub>2</sub>), 134.4 (d,  $J_{PC} = 29.8$  Hz, PPh<sub>2</sub>), 136.1 (d,  $J_{PC} = 9.8$  Hz, PPh<sub>2</sub>), 147.0 (d,  $^2J_{PC} = 76.3$  Hz,  $CCO_2Me$ ), 150.0 (d,  $J_{PC} = 59.0$  Hz, PPh<sub>2</sub>), 162.2 (d,  $^2J_{PC} = 20.8$  Hz, PPh<sub>2</sub>), 203.1 (d,  $^1J_{PC} = 32.6$  Hz,  $C(O)PPh_2$ ), 204.3 (d,  $^3J_{PC} = 1.4$  Hz,  $CO_2Me$ ), 218.0 (d,  $^2J_{PC} = 26.4$  Hz, CO), 253.3 (d,  $^2J_{PC} = 24.0$  Hz, CH). Mass (FAB, Xe, *m*-nitrobenzyl alcohol matrix) *m/z* 517 ( $M^+ + 1$ , 40.2), 485 ( $M^+ - OMe$ , 68.5), 460 ( $M^+ - 2CO$ , 93.8), 401 ( $M^+ - 2CO - CO_2Me$ , 50.2), 376 ( $(C_5Me_5)FePPh_2$ , 100). Exact mass calcd for  $C_{28}H_{29}FeO_4P$ : 516.1143. Found: 516.1150.

### 3.6. Reaction of $(\eta^5-C_5Me_5)Fe_2(CO)_4(\mu-CO)(\mu-PPh_2)$ (**1**) with $PhC\equiv CH$

A solution of **1** (62 mg, 0.11 mmol) and  $PhC\equiv CH$  (95% purity by GC, 13  $\mu$ l, 0.13 mmol) in benzene (10 ml) was stirred for 9 h at 40 °C. The resulting solution was filtered through a Celite pad (activated in an oven at 180 °C for several days) and the filtrate was evaporated to dryness under reduced pressure. The black residue was layered with pentane and kept at room temperature for 5 days. Black crystals of  $(\eta^5-C_5Me_5)Fe_2(CO)_3(\mu-CO)[\mu-CH=CPhC(O)PPh_2]$  (**4c**) (45 mg) was isolated from the solution. The mother liquor was again kept at room temperature to afford 4 mg of **4c**. The total yield of **4c** was 67% (49 mg, 0.073 mmol). The mother liquor was then cooled to 5 °C to give orange crystals of  $(\eta^5-C_5Me_5)Fe(CO)[CH=CPhC(O)PPh_2]$  (**6c**) in 5% yield (3 mg, 0.006 mmol).

The reaction of **1** with  $PhC\equiv CH$  was monitored by  $^1H$  and  $^{31}P$  NMR spectroscopy. A benzene-*d*<sup>6</sup> solution of **1** and  $PhC\equiv CH$  in an NMR tube was heated at 40 °C. After 12 h, the  $^1H$  NMR spectrum showed only the signals of **4c** and excess  $PhC\equiv CH$ . The temperature was raised to 60 °C and the heating was continued. After 1 day, the  $^1H$  NMR spectrum showed the signals of **4c** and  $(\eta^5-C_5Me_5)_2Fe_2(CO)_4$  as major products, together with signals arising from some unidentified minor products. The  $^1H$  and  $^{31}P$  NMR, and IR spectral data for **4c** and **6c** are listed in Table 3. **4c**:  $^{13}C$  NMR (75.5 MHz,  $C_6D_6$ )  $\delta$  9.2 ( $C_5Me_5$ ), 81.7 (d,  $^2J_{PC} = 77.7$  Hz,  $CPh$ ), 96.2 ( $C_5Me_5$ ), 127.2 (Ph), 128.9 (Ph), 130.2 (br, PPh<sub>2</sub>), 131.0 (Ph), 132.6 (d,  $J_{PC} = 8.9$  Hz, PPh<sub>2</sub>), 132.8 (Ph), 134.5 (d,  $J_{PC} = 7.5$  Hz, PPh<sub>2</sub>), 142.5 (d,  $J_{PC} = 10.7$  Hz, PPh<sub>2</sub>), 168.1 (d,  $^2J_{PC} = 21.2$  Hz,  $\mu-CH$ ), 199.7 (d,  $^1J_{PC} = 38.3$  Hz,  $-C(O)PPh_2-$ ), 213.7 (CO), 239.2 (d,

$^2J_{PC} = 25.9$  Hz,  $\mu$ -CO). Mass (FAB, Xe, *m*-nitrobenzyl alcohol matrix)  $m/z$  675 ( $M^+ + 1$ , 50.0), 646 ( $M^+ - CO$ , 4.8), 618 ( $M^+ - 2CO$ , 100), 590 ( $M^+ - 3CO$ , 81.4), 562 ( $M^+ - 4CO$ , 33.0), 534 ( $M^+ - 5CO$ , 69.5). Anal. Calcd for  $C_{35}H_{31}Fe_2O_5P$ : C, 62.34; H, 4.63. Found: C, 61.83; H, 4.61. **6c**:  $^{13}C$  NMR (75.5 MHz,  $C_6D_6$ )  $\delta$  9.6 ( $C_5Me_5$ ), 93.8 ( $C_5Me_5$ ), 126.6 (Ph), 126.7 (d,  $J_{PC} = 0.8$  Hz,  $PPh_2$ ), 127.9, 128.1, 128.4, 128.5 (Ph or  $PPh_2$ ), 129.6 (d,  $J_{PC} = 2.5$  Hz,  $PPh_2$ ), 131.1 (d,  $J_{PC} = 2.4$  Hz,  $PPh_2$ ), 131.2, 131.7 (Ph), 132.5 (d,  $J_{PC} = 8.4$  Hz,  $PPh_2$ ), 135.6 (d,  $J_{PC} = 30.3$  Hz,  $PPh_2$ ), 136.2 (d,  $J_{PC} = 10.0$  Hz,  $PPh_2$ ), 155.5 (d,  $J_{PC} = 71.1$  Hz, CPh), 206.5 (dd ( $^1H$  nondecoupling mode),  $^2J_{PC} = 70.8$  Hz,  $^3J_{CH} = 15.6$  Hz  $-C(O)PPh_2$ ), 218.8 (d,  $^2J_{PC} = 27.0$  Hz, CO), 231.3 (dd ( $^1H$  nondecoupling mode),  $^2J_{PC} = 25.3$  Hz,  $^1J_{CH} = 136.6$  Hz, CH). Mass (FAB, Xe, *m*-nitrobenzyl alcohol matrix)  $m/z$  534 ( $M^+ + 1$ , 36.4), 506 ( $M^+ - CO$ , 10.7), 478 ( $M^+ - 2CO$ , 43.9), 404 ( $M^+ - CO - HCCPh$ , 29.0), 376 ( $(C_5Me_5)FePPh_2$ , 100).

### 3.7. Reaction of $(\eta^5-C_5Me_5)Fe_2(CO)_4(\mu-CO)(\mu-PPh_2)$ (**1**) with $MeO_2CC\equiv CCO_2Me$

A solution of **1** (80 mg, 0.14 mmol) and  $MeO_2CC\equiv CCO_2Me$  (40 mg, 0.28 mmol) in benzene (20 ml) was stirred for 12 h at 50 °C. The solution was filtered through a Celite pad. After removal of volatiles, the brown residue was dissolved in a minimum amount of benzene. The solution was layered with hexane and kept at 5 °C for several days to give  $(\eta^5-C_5Me_5)Fe(CO)[C(CO_2Me)=C(CO_2Me)C(O)PPh_2]$  (**6d**) as orange crystals in 30% yield (24 mg, 0.042 mmol). The  $^1H$  and  $^{31}P$  NMR, and IR spectral data for **6d** are listed in Table 3. **6d**:  $^{13}C$  NMR (75.5 MHz,  $C_6D_6$ )  $\delta$  9.3 ( $C_5Me_5$ ), 51.69 ( $CO_2Me$ ), 51.72 ( $CO_2Me$ ), 95.1 (d,  $J_{PC} = 1.1$  Hz,  $C_5Me_5$ ), 130.3 (d,  $J_{PC} = 2.2$  Hz,  $PPh_2$ ), 130.6 (d,  $J_{PC} = 46.3$  Hz,  $PPh_2$ ), 131.4 (d,  $J_{PC} = 2.3$  Hz,  $PPh_2$ ), 132.4 (d,  $J_{PC} = 13.2$  Hz,  $PPh_2$ ), 132.9 (d,  $J_{PC} = 36.9$  Hz,  $PPh_2$ ), 135.3 (d,  $J_{PC} = 11.8$  Hz,  $PPh_2$ ), 145.5 (d,  $J_{PC} = 28.7$  Hz,  $C(O)PPh_2$ ), 165.7 (d,  $J_{PC} = 1.2$  Hz,  $CO_2Me$ ), 166.5 (d,  $J_{PC} = 14.2$  Hz,  $C(CO_2Me)$ ), 166.9 (d,  $J_{PC} = 3.6$  Hz,  $CO_2Me$ ), 219.3 (d,  $^2J_{PC} = 26.1$  Hz, CO), 258.6 (d,  $^2J_{PC} = 12.8$  Hz,  $Fe=C(CO_2Me)$ ). Mass (FAB, Xe, *m*-nitrobenzyl alcohol matrix)  $m/z$  575 ( $M^+ + 1$ , 70.9), 518 ( $M^+ - 2CO$ , 100), 459 ( $M^+ - 2CO - CO_2Me$ , 57.8), 376 ( $(C_5Me_5)FePPh_2$ , 46.9). Exact mass calcd. for  $C_{30}H_{31}FeO_6P$ : 574.1208. Found: 574.1200.

### 3.8. Reaction of $(\eta^5-C_5Me_5)Fe_2(CO)_4(\mu-CO)[\mu-CH=CHC(O)PPh_2]$ (**4a**) with $HC\equiv CH$

Acetylene gas was bubbled through a solution of **4a** (100 mg, 0.175 mmol) in benzene (10 ml) for 3 h at 40 °C. The resulting solution contained unreacted **4a** and **6a** in a 1:1 ratio together with trace amount of

**5a**, which were confirmed by the TLC and  $^1H$  NMR spectroscopy.

### 3.9. Thermal decomposition of **4a** or **4c**

A solution of **4a** (5.0 mg,  $8.4 \times 10^{-3}$  mmol) in  $C_6D_6$  (0.5 ml) in a sealed NMR tube was heated at 60 °C for 3 days. The  $^1H$  NMR spectrum of the resulting solution showed the signals of **6a** as a main product. Similarly, heating of a  $C_6D_6$  solution of **4c** at 60 °C gave **6c** as a main product after several days.

### 3.10. X-ray crystal structure analysis

Each of the crystals of **1**, **4c**, **5b**, and **6a** for X-ray diffraction study was cut down to the suitable size and mounted on a glass rod. Intensity data were collected by a Rigaku AFC-6A four-circle diffractometer with graphite-monochromated Mo  $K\alpha$  radiation at 18 °C. Diffraction data were collected in the  $\omega$ - $2\theta$  or  $\omega$  scan mode. The structures of **1**, **4c**, and **6a** were solved by direct methods (program MALTAN 71 [32] for **1**, program RANTAN 81 [32] for **4c** and **6a**) and refined by the block-diagonal least-squares method with individual anisotropic thermal parameters for non-hydrogen atoms. The positions of hydrogen atoms on the phenyl groups for **1** and **4c** were calculated and added to the structure factor calculations without refinement. The positions of hydrogen atoms for methine and phenyl groups for **6a** were calculated and added to the structure factor calculations without refinement. The structure of **5b** was solved by the heavy-atom method. The positions of two iron atoms and a phosphorus atom were deduced from Patterson syntheses and the remaining non-hydrogen atoms were found by subsequent difference Fourier syntheses and refined by the block-diagonal least-squares method with individual anisotropic thermal parameters. The positions of two hydrogen atoms for methine groups were found by difference Fourier syntheses and refined with isotropic thermal parameters. The positions of hydrogen atoms on the phenyl groups were calculated and added to the structure factor calculations without refinement. All the calculations were performed on a Nippon Electric Co. ACOS-2000 computer system at the Computer Center of Tohoku University with the Universal Program System UNICS III [33]. Crystallographic data for **1**, **4c**, **5b**, and **6a** are summarized in Table 3. Crystallographic Information has been deposited with the Cambridge Crystallographic Data Centre (CCDC Nos. 211274 (**1**), 211275 (**4c**), 211276 (**5b**), and 211277 (**6a**)). The data can be obtained free of charge via [www.ccdc.cam.ac.uk](http://www.ccdc.cam.ac.uk) (or from the Cambridge Crystallographic Data Centre, 12 Union Road, Cambridge CB21EZ, UK; fax: (+44)1223-336-033; or [deposit@ccdc.cam.ac.uk](mailto:deposit@ccdc.cam.ac.uk)).

## Acknowledgements

This work was supported by Grants-in-Aid for Scientific Research (Nos. 14044010 and 14078202) from the Ministry of Education, Culture, Sports, Science and Technology, Japan.

## References

- [1] For reviews, see, for instance: (a) D.A. Roberts, G.L. Geoffroy, in: G. Wilkinson, F.G.A. Stone, E.W. Abel (Eds.), *Comprehensive Organometallic Chemistry*, Pergamon Press, Oxford, 1982, Chapter 40; (b) M.J. Chetcuti, in: E.W. Abel, F.G.A. Stone, G. Wilkinson (Eds.), *Comprehensive Organometallic Chemistry II*, Pergamon Press, Oxford, 1995, Chapter 2.
- [2] H. Hashimoto, H. Tobita, H. Ogino, *Organometallics* 12 (1993) 2182.
- [3] (a) H. Hashimoto, H. Tobita, H. Ogino, *J. Organomet. Chem.* 499 (1995) 205; (b) H. Hashimoto, Ph.D. Thesis, Tohoku University, 1995.
- [4] (a) R. Zolk, H. Werner, *J. Organomet. Chem.* 252 (1983) C53; (b) H. Werner, R. Zolk, *Organometallics* 4 (1985) 601; (c) H. Werner, R. Zolk, *Chem. Ber.* 120 (1987) 1003; (d) R. Zolk, H. Werner, *J. Organomet. Chem.* 331 (1987) 95; (e) B. Klingert, A.L. Rheingold, H. Werner, *Inorg. Chem.* 27 (1988) 1354.
- [5] (a) A.J.M. Caffyn, J.M. Mays, G.A. Solan, *Organometallics* 12 (1993) 1876; (b) A. Martin, M.J. Mays, P.R. Raithby, G.A.I. Solan, *J. Chem. Soc., Dalton Trans.* (1993) 355; (c) A.J. Edwards, A. Martin, M.J. Mays, D. Nazar, P.R. Raithby, G.A. Solan, *J. Chem. Soc., Dalton Trans.* (1993) 1789; (d) A.J. Edwards, M.J. Mays, P.R. Raithby, G.A. Solan, *Organometallics* 15 (1996) 4085; (e) N. Choi, G. Conole, M. Kessler, J.D. King, M.J. Mays, M. McPartlin, G.E. Pateman, G.A. Solan, *J. Chem. Soc., Dalton Trans.* (1999) 3941; (f) J.D. King, M.J. Mays, C.-Y. Mo, P.R. Raithby, M.A. Rennie, G.A. Solan, T. Adatia, G. Conole, *J. Organomet. Chem.* 601 (2000) 271.
- [6] (a) K. Yasufuku, H. Yamazaki, *J. Organomet. Chem.* 35 (1972) 367; (b) K. Yasufuku, K. Aoki, H. Yamazaki, *J. Organomet. Chem.* 84 (1975) C28; (c) B.L. Barnett, C. Krüger, *Cryst. Struct. Commun.* 2 (1973) 347.
- [7] (a) R. Regragui, P.H. Dixneuf, N.J. Taylor, A.J. Carty, *Organometallics* 3 (1984) 814; (b) R. Regragui, P.H. Dixneuf, N.J. Taylor, A.J. Carty, *Organometallics* 9 (1990) 2234.
- [8] (a) W.F. Smith, N.J. Taylor, A.J. Carty, *J. Chem. Soc., Chem. Commun.* (1976) 896; (b) A.D. Horton, M.J. Mays, P.R. Raithby, *J. Chem. Soc., Chem. Commun.* (1985) 247; (c) A.D. Horton, A.C. Kemball, M.J. Mays, *J. Chem. Soc., Dalton Trans.* (1988) 2953; (d) D. Braga, A.J.M. Caffyn, M.C. Jennings, M.J. Mays, L. Manojlovic-Muir, P.R. Raithby, P. Sabatino, K.W. Woulfe, *J. Chem. Soc., Chem. Commun.* (1989) 1401; (e) L. Manojlovic-Muir, M.J. Mays, K.W. Woulfe, *J. Chem. Soc., Dalton Trans.* (1992) 1531; (f) A.J.M. Caffyn, M.J. Mays, G.A. Solan, G. Conole, A. Tiripicchio, *J. Chem. Soc., Dalton Trans.* (1993) 2345.
- [9] (a) R.J. Haines, C.R. Nolte, R. Greatrex, N.N. Greenwood, *J. Organomet. Chem.* 26 (1971) C45; (b) R.J. Haines, C.R. Nolte, *J. Organomet. Chem.* 36 (1972) 163.
- [10] K. Yasufuku, H. Yamazaki, *J. Organomet. Chem.* 28 (1971) 415.
- [11] P.E. Garrou, *Chem. Rev.* 81 (1981) 229.
- [12] (a) S.-G. Shyu, P.-J. Lin, Y.-S. Wen, *J. Organomet. Chem.* 443 (1993) 115; (b) S.-G. Shyu, J.-Y. Hsu, Y.-S. Wen, *J. Organomet. Chem.* 453 (1993) 97; (c) S.-G. Shyu, P.-J. Lin, T.-Y. Dong, Y.-S. Wen, *J. Organomet. Chem.* 460 (1993) 229; (d) S.-G. Shyu, J.-Y. Hsu, P.-J. Lin, W.-J. Wu, S.-M. Peng, G.-H. Lee, Y.-S. Wen, *Organometallics* 13 (1994) 1699.
- [13] (a) R.J. Doedens, W.T. Robinson, J.A. Ibers, *J. Am. Chem. Soc.* 89 (1967) 4323; (b) H. Brunner, H. Peter, *J. Organomet. Chem.* 393 (1990) 411; (c) H. Brunner, H. Peter, *J. Organomet. Chem.* 425 (1992) 119; (d) P. Leoni, M. Pasquali, M. Sommovigo, A.F. Albinati, P. Lianza, S. Pregosin, H. Ruegger, *Organometallics* 13 (1994) 4017.
- [14] (a) W. Ehrl, H. Vahrenkamp, *J. Organomet. Chem.* 63 (1973) 389; (b) H. Vahrenkamp, *J. Organomet. Chem.* 63 (1973) 399.
- [15] J.R. Huntsman, L.F. Dahl, unpublished work quoted in Clegg, W. *Inorg. Chem.* 15 (1976) 1609.
- [16] G.L. Borgne, R. Mathieu, *J. Organomet. Chem.* 208 (1981) 201.
- [17] We have recently synthesized a Ru–Fe mixed metal analog of **3**,  $(\eta^5\text{-C}_5\text{Me}_5)_2\text{RuFe}(\text{CO})_3(\mu\text{-PPh}_2)[\mu\text{-CH}=\text{CPhC}(\text{O})]$ , and succeeded in its X-ray crystal structure determination. Based on the spectral similarities between this complex and **3**, we suggest the structure of **3** as shown in Eq. (2). The structure of the Ru–Fe analog of **3** will be reported elsewhere.
- [18] S.A. Knox, B.R. Lloyd, D.A.V. Morton, A.G. Orpen, M.L. Turner, G. Hogarth, *Polyhedron* 14 (1995) 2723.
- [19] S.D. Ittel, J.A. Ibers, *Adv. Organomet. Chem.* 14 (1976) 33.
- [20] C.M. Lukehart, *Fundamental Transition Metal Organometallic Chemistry*, Brooks, Cole, Monterey, California, 1985, pp. 41.
- [21] F.A. Cotton, G. Wilkinson, *Advanced Inorganic Chemistry*, fifth ed., Wiley, 1988, pp. 1031.
- [22] M. Akita, N. Ishii, A. Takabuchi, M. Tanaka, Y. Moro-oka, *Organometallics* 13 (1994) 258.
- [23] W. Fresenius, J.F.K. Huber, E. Pungler, G.A. Rechnitz, W. Simon, T.S. West, in: E. Pretsch, T. Clere, J. Seibl, W. Simon (Eds.), *Tables of Spectral Data for Structure Determination of Organic Compounds*, second ed., Springer, Berlin, 1989.
- [24] M.T. Ashby, J.H. Enemark, *Organometallics* 6 (1987) 1323.
- [25] H. Adams, N.A. Bailey, A.N. Day, M.J. Morris, M.M. Harrison, *J. Organomet. Chem.* 407 (1991) 247.
- [26] A.J.M. Caffyn, M.J. Mays, G.A. Solan, A. Tiripicchio, *J. Chem. Soc., Dalton Trans.* (1993) 2345.
- [27] H. Adams, N.A. Bailey, P. Blenkinsop, M.J. Morris, *J. Chem. Soc., Dalton Trans.* (1997) 3589.
- [28] J.G. Smith, D.T. Thompson, *J. Chem. Soc. (A)* (1967) 1694.
- [29] R.B. King, F.G.A. Stone, *Inorg. Synth.* 7 (1963) 110.
- [30]  $\text{PhC}\equiv\text{CH}$  was prepared analogously to  $\text{PhC}\equiv\text{CPh}$ ; L.I. Smith, M.M. Folkoff, *Org. Synth.* 3 (1955) 350.
- [31] W.L. Collier, R.S. Macomber, *J. Org. Chem.* 38 (1973) 1369.
- [32] (a) Y. Jia-Xing, *Acta Crystallogr. Sect. A* 37 (1981) 642; (b) Y. Jia-Xing, *Acta Crystallogr., Sect. A* 39 (1983) 35.
- [33] T. Sakurai, M. Kobayashi, *Rikagaku Kenkyuusho Hokoku* 55 (1979) 69.